

Supporting Information

Photoluminescence of Ag(I) complexes with square-planar coordination geometry: the first observation

Alexander V. Artem'ev,^{*a,b} Maxim R. Ryzhikov,^{a,b} Alexey S. Berezin,^a Ilya E. Kolesnikov,^c Denis G. Samsonenko,^{a,b} Irina Yu. Bagryanskaya^{b,d}

^a Nikolaev Institute of Inorganic Chemistry, Siberian Branch of Russian Academy of Sciences, 3, Acad. Lavrentiev Ave., Novosibirsk 630090, Russian Federation

^b Novosibirsk State University, 2, Pirogova Str., Novosibirsk 630090, Russian Federation

^c Center for Optical and Laser Materials Research, Saint Petersburg State University, Ulianovskaya, 5, Saint Petersburg 198504, Russian Federation

^d N. N. Vorozhtsov Novosibirsk Institute of Organic Chemistry, Siberian Branch of Russian Academy of Sciences, 9, Acad. Lavrentiev Ave., Novosibirsk 630090, Russian Federation

*Author for correspondence: chemisufarm@yandex.ru (Alexander V. Artem'ev)

Table of Contents

Pages

S2	§1. General remarks
S2–3	§2. Synthetic procedures
S3–6	§3. X-Ray crystallography
S7	§4. TG, DTG and c-DTA curves
S8	§5. FT-IR spectra
S8–9	§6. ESI-MS spectra
S9–14	§7. NMR spectra
S14–26	§8. Computational details
S26–32	§9. Photophysical data
S33	§10. References

§1. General remarks

AgClO4 (97%, Alfa Aesar), AgOTf (98%, Alfa Aesar), AgBF4 (99%, Alfa Aesar) and MeCN (HPLC grade, Cryochrom) were commercial products. Tris(2-pyridyl)phosphine (Py3PO) was prepared by oxidation of the corresponding phosphine [1] with H2O2 in a H2O/acetone system.

^1H (500.13 MHz) and $^{31}\text{P}\{\text{H}\}$ NMR (202.47 MHz) spectra were recorded on a Bruker Advance 500 spectrometer. Chemical shifts were reported in δ (ppm) relative to CD3CN [or (CD3)2CO] residual peak (^1H) as an internal standard or H3PO4 (^{31}P) as an external standard. FT-IR spectra were collected on a Bruker Vertex 80 spectrometer. The microanalyses were performed on a MICRO cube analyzer. XRPD analyses were performed on a Shimadzu XRD-7000 diffractometer (Cu- $\text{K}\alpha$ radiation, Ni – filter, 3–35° 2θ range, 0.03° 2θ step, 5s per point). ESI-MS spectra were recorded using a LC/MS quadrupole Agilent 6130 mass-spectrometer. Thermogravimetric analyses were carried out in a closed Al2O3 pan under helium flow at 10 °C/min $^{-1}$ heating rate using a Netzsch STA 449 F1 Jupiter STA.

§2. Synthetic procedures

General procedure for synthesis of 1–3. To a mixture of tris(2-pyridyl)phosphine oxide (141 mg, 0.50 mmol) and a Ag(I) salt (0.25 mmol), acetonitrile (1.5 mL) was added. The suspension was stirred at ambient temperature until the dissolution of precipitate (about 5 min), and then Et2O (5 mL) was added to a resulting solution. The precipitated powder of **1–3** was additionally washed with Et2O (1 x 3 mL) and dried under vacuum.

[Ag(Py₃PO)₂]ClO₄ (1). Yield: 164 mg (85%). White powder, poorly soluble in water. Anal. Calcd for C30H24AgClN6O6P2 (769.82): C, 46.8; H, 3.1; N, 10.9. Found: C, 46.8; H, 3.1; N, 10.8. ^1H NMR (500.13 MHz, CD3CN, 23 °C) δ 8.47 (ddd, J = 4.9, 1.8, 1.0 Hz, 6H), 8.31 (ddt, J = 7.6, 6.3, 1.1 Hz, 6H), 8.02 (tdd, J = 7.8, 3.9, 1.7 Hz, 6H), 7.51 (dddd, J = 7.8, 4.9, 2.3, 1.3 Hz, 6H). $^{31}\text{P}\{\text{H}\}$ NMR (202.47 MHz, CD3CN, 23 °C) δ 2.94. FT-IR: ν = 405 (m), 422 (s), 430 (m), 465 (m), 480 (vs), 509 (s), 527 (vs), 621 (w), 631 (m), 710 (w), 727 (m), 746 (s), 770 (vs), 781 (s), 793 (s), 887 (w), 982 (m), 989 (m), 1001 (s), 1045 (w), 1086 (m), 1126 (w), 1152 (m), 1238 (w), 1273 (w), 1283 (w), 1292 (w), 1414 (s), 1422 (s), 1429 (s), 1449 (vs), 1560 (s), 1574 (vs), 2955 (w), 2976 (w), 3034 (m), 3053 (w) cm $^{-1}$.

[Ag(Py₃PO)₂]OTf (2). Yield: 168 mg (82%). White powder, soluble in water. Anal. Calcd for C31H24AgF3N6O5P2S (819.43): C, 45.4; H, 2.9; N, 10.3. Found: C, 45.3; H, 3.0; N, 10.3. ^1H NMR (500.13 MHz, CD3CN, 23 °C) δ 8.47 (ddd, J = 4.9, 1.7, 0.9 Hz, 6H), 8.31 (ddt, J = 7.6, 6.3, 1.1 Hz, 6H), 8.02 (tdd, J = 7.8, 3.9, 1.7 Hz, 6H), 7.51 (dddd, J = 7.8, 4.9, 2.2, 1.3 Hz, 6H). $^{31}\text{P}\{\text{H}\}$ NMR (202.47 MHz, CD3CN, 23 °C) δ 2.78. FT-IR: ν = 501 (m), 517 (m), 546 (vs), 625 (w), 638 (s), 739 (m), 748 (s), 766 (m), 779 (m), 989 (m), 995 (m), 1034 (s), 1086 (m), 1124 (m), 1144 (s), 1211 (s), 1281 (s), 1427 (s), 1454 (m), 1576 (s), 2995 (vw), 3046 (w), 3055 (w), 3082 (w) cm $^{-1}$.

[Ag(Py₃PO)₂]BF₄ (3). Yield: 168 mg (89%). White powder, soluble in water. Anal. Calcd for C30H24AgBF4N6O2P2 (757.17): C, 47.6; H, 3.2; N, 11.1. Found: C, 47.5; H, 3.2; N, 11.2. ^1H NMR (500.13 MHz, CD3CN, 23 °C) δ 8.49 (d, J = 4.8 Hz, 6H), 8.37–8.30 (m, 6H), 8.04 (tdd, J = 7.8, 3.9, 1.6

Hz, 6H), 7.55–7.50 (m, 6H). $^{31}\text{P}\{\text{H}\}$ NMR (202.47 MHz, CD₃CN, 23 °C) δ 1.61. FT-IR: ν = 399 (w), 447 (m), 457 (m), 501 (m), 548 (vs), 621 (w), 748 (s), 779 (m), 849 (w), 989 (s), 1038 (s), 1059 (s), 1086 (s), 1123 (s), 1148 (s), 1211 (s), 1285 (m), 1425 (s), 1454 (m), 1574 (s), 1649 (w), 2992 (vw), 3046 (w) cm⁻¹.

§3. X-Ray crystallography

For preparation of single crystals of **1–3**, the as-synthesized powders (~ 10 mg) were dissolved in water (~ 1 mL), and the resulting solutions were slowly evaporated at room temperature for several days. Diffraction data for single-crystals of **1** and **2** were obtained on an automated Agilent Xcalibur diffractometer equipped with an area AtlasS2 detector (graphite monochromator, $\lambda(\text{MoK}\alpha)$ = 0.71073 Å, ω-scans). Integration, absorption correction, and determination of unit cell parameters were performed using the CrysAlisPro program package [2]. The data for crystals of **3** were collected on a Bruker Kappa Apex II CCD diffractometer using φ,ω-scans of narrow (0.5°) frames with MoKα radiation (λ = 0.71073 Å) and a graphite monochromator. The structures were solved by dual space algorithm (SHELXT [3]) and refined by the full-matrix least squares technique (SHELXL [4]) in the anisotropic approximation (except hydrogen atoms). Positions of hydrogen atoms of organic ligands were calculated geometrically and refined in the riding model. The [ClO₄]⁻ and [OTf]⁻ anions within **1** and **2**, respectively, are disordered over two orientations around the inversion center.

The crystallographic data and details of the structure refinements are summarized in Table S1. CCDC 1858730–1858732 and 1896382 contain the supplementary crystallographic data for this paper. These data can be obtained free of charge from The Cambridge Crystallographic Data Center at http://www.ccdc.cam.ac.uk/data_request/cif.

Table S1. Crystal data and structure refinement for **1-RT**, **1-LT**, **2** and **3**.

	1-RT	1-LT	2	3
CCDC	1858730	1858731	1858732	1896382
Empirical formula	C ₃₀ H ₂₄ AgClN ₆ O ₆ P ₂	C ₃₀ H ₂₄ AgClN ₆ O ₆ P ₂	C ₃₁ H ₂₄ AgF ₃ N ₆ O ₅ P ₂ S	C ₃₀ H ₂₄ AgBF ₄ N ₆ O ₂ P ₂
M, g/mol	769.81	769.81	819.43	757.17
T, K	295(2)	130(2)	130(2)	296
Crystal system	<i>Monoclinic</i>	<i>Monoclinic</i>	<i>Monoclinic</i>	<i>Triclinic</i>
Space group	<i>P2₁/n</i>	<i>P2₁/n</i>	<i>P2₁/n</i>	<i>P-1</i>
a, Å	8.6372(6)	8.5466(3)	8.8857(4)	9.3435(7)
b, Å	15.7157(9)	15.6404(4)	15.5795(6)	9.9903(8)
c, Å	12.0166(8)	11.9157(4)	12.0439(5)	17.8533(15)
α, deg.	90.000	90.000	90.000	81.010(5)
β, deg.	106.087(7)	105.930(4)	107.786(5)	88.125(5)
γ, deg.	90.000	90.000	90.000	82.406(4)
V, Å ³	1567.26(18)	1531.63(9)	1587.60(12)	1631.5(2)
Z	2	2	2	2
D(calc.), g/cm ³	1.631	1.669	1.714	1.541
μ, mm ⁻¹	0.884	0.905	0.872	0.777
F(000)	776	776	824	760
Crystal size, mm	0.29 × 0.22 × 0.18	0.36 × 0.24 × 0.20	0.42 × 0.35 × 0.35	0.80 × 0.40 × 0.25
θ range for data collection, deg.	3.39–29.62	3.42–29.63	3.40–29.12	2.30–55.34
Index ranges	-10 ≤ h ≤ 11, -19 ≤ k ≤ 19, -15 ≤ l ≤ 13	-11 ≤ h ≤ 10, -21 ≤ k ≤ 21, -16 ≤ l ≤ 15	-11 ≤ h ≤ 12, -19 ≤ k ≤ 20, -15 ≤ l ≤ 8	-12 ≤ h ≤ 12, -12 ≤ k ≤ 12, -23 ≤ l ≤ 22
Reflections collected / independent	12110 / 3743	12438 / 3769	7919 / 3549	25068 / 5562
R _{int}	0.0186	0.0217	0.0164	0.028
Reflections with I > 2σ(I)	3219	3276	3244	7411
Goodness-of-fit on F ²	1.071	1.069	1.126	1.045
Final R indices [I > 2σ(I)]	R ₁ = 0.0430, wR ₂ = 0.1284	R ₁ = 0.0412, wR ₂ = 0.1162	R ₁ = 0.0274, wR ₂ = 0.0597	R ₁ = 0.0515, wR ₂ = 0.1598
R indices (all data)	R ₁ = 0.0500, wR ₂ = 0.1344	R ₁ = 0.0477, wR ₂ = 0.1220	R ₁ = 0.0313, wR ₂ = 0.0611	R ₁ = 0.0668, wR ₂ = 0.1735
Largest diff. peak / hole, e/Å ³	0.843 / -1.206	1.275 / -1.754	0.401 / -0.362	1.74 / -0.64

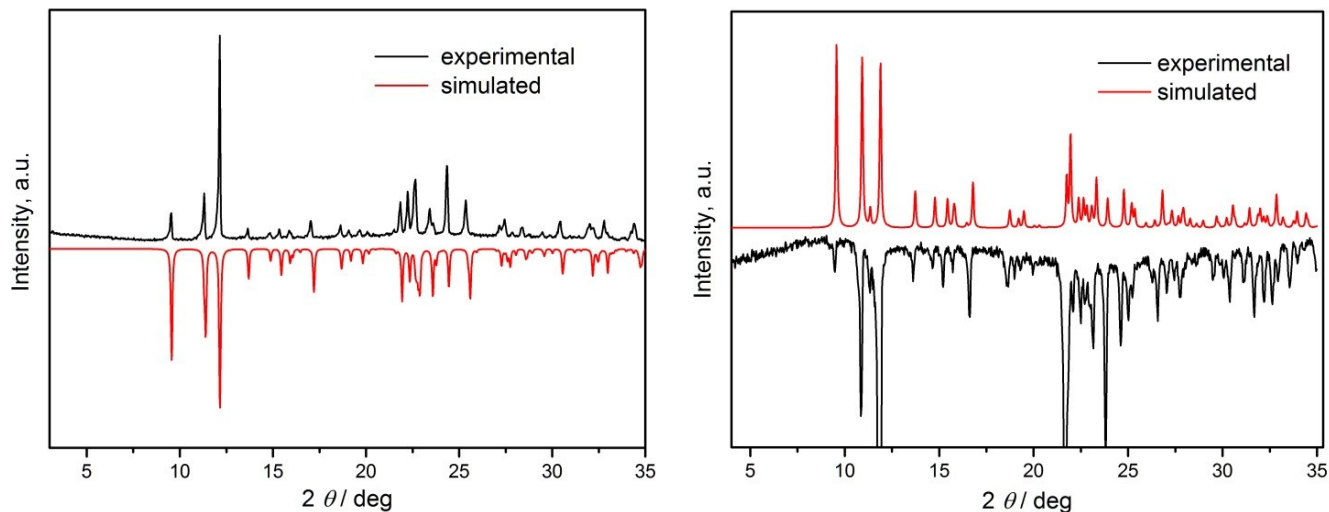


Fig. S1. Experimental and simulated XRPD patterns for “as-synthesized” samples of **1** (left) and **2** (right).

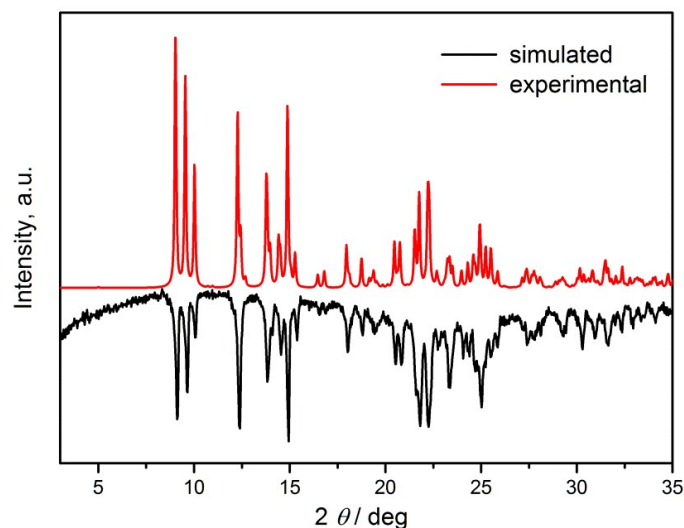


Fig. S2. Experimental and simulated XRPD patterns for “as-synthesized” sample of **3**.

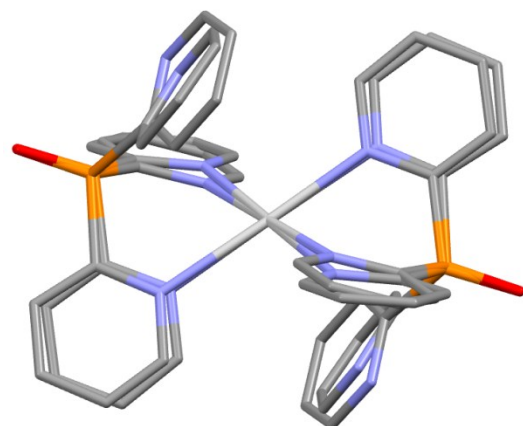


Fig. S3. Overplayed $[\text{Ag}(\text{N},\text{N}'-\text{Py}_3\text{PO})_2]^+$ cations of **1** and **3** (the H atoms are omitted).

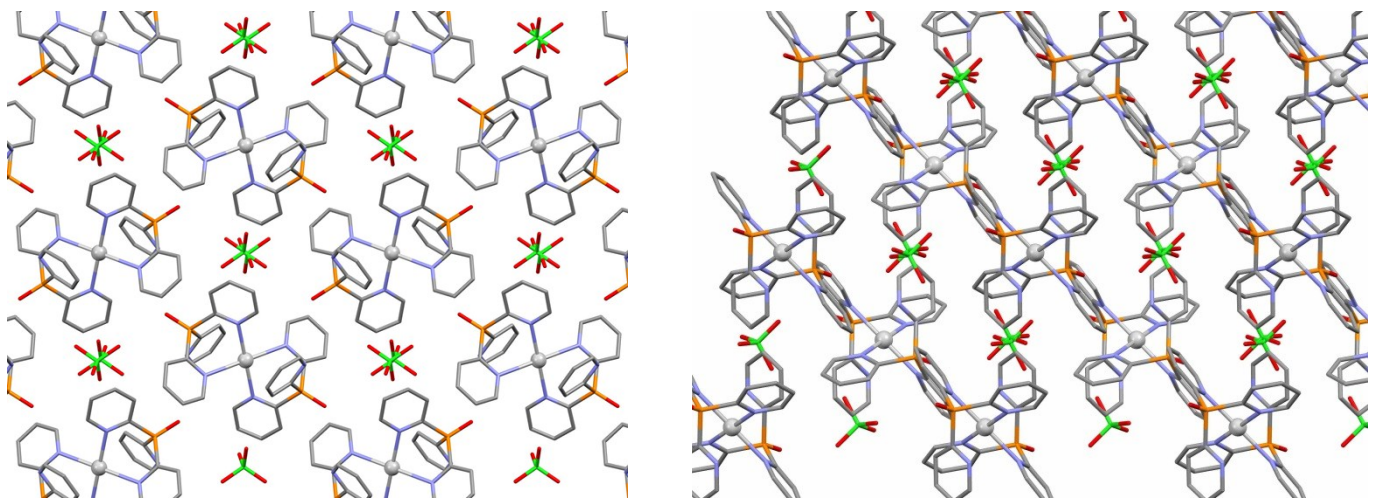


Fig. S4. Perspective view of crystal packing of **1** along *a* (left) and *b* axes (the H atoms are omitted).

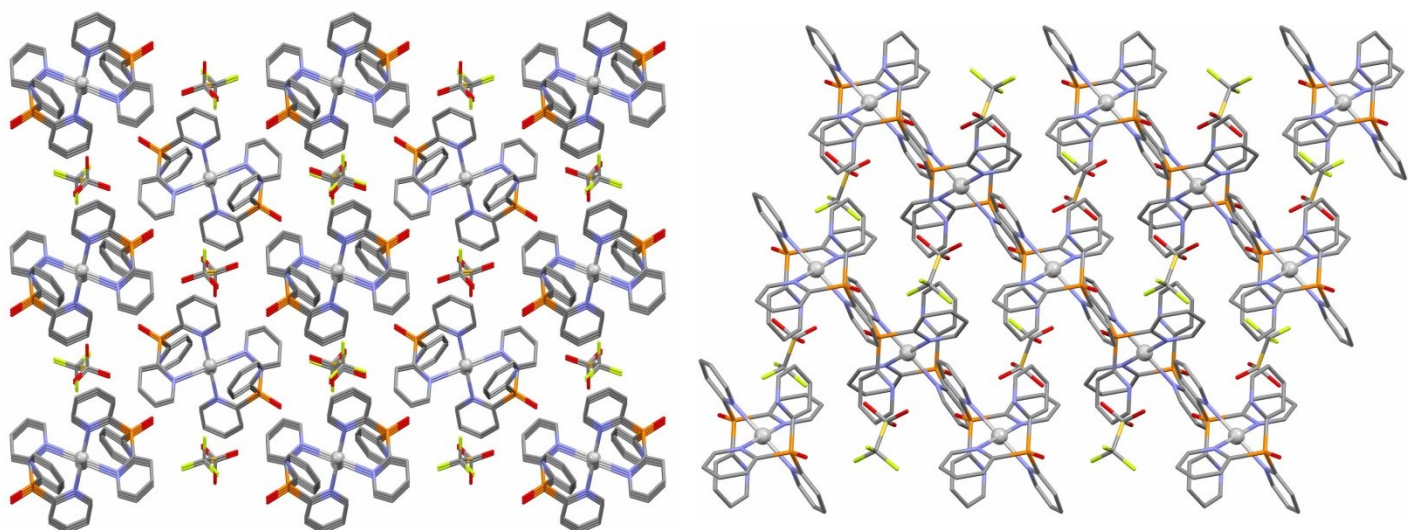


Fig. S5. Perspective view of crystal packing of **2** along *a* (left) and *b* axes (the H atoms are omitted).

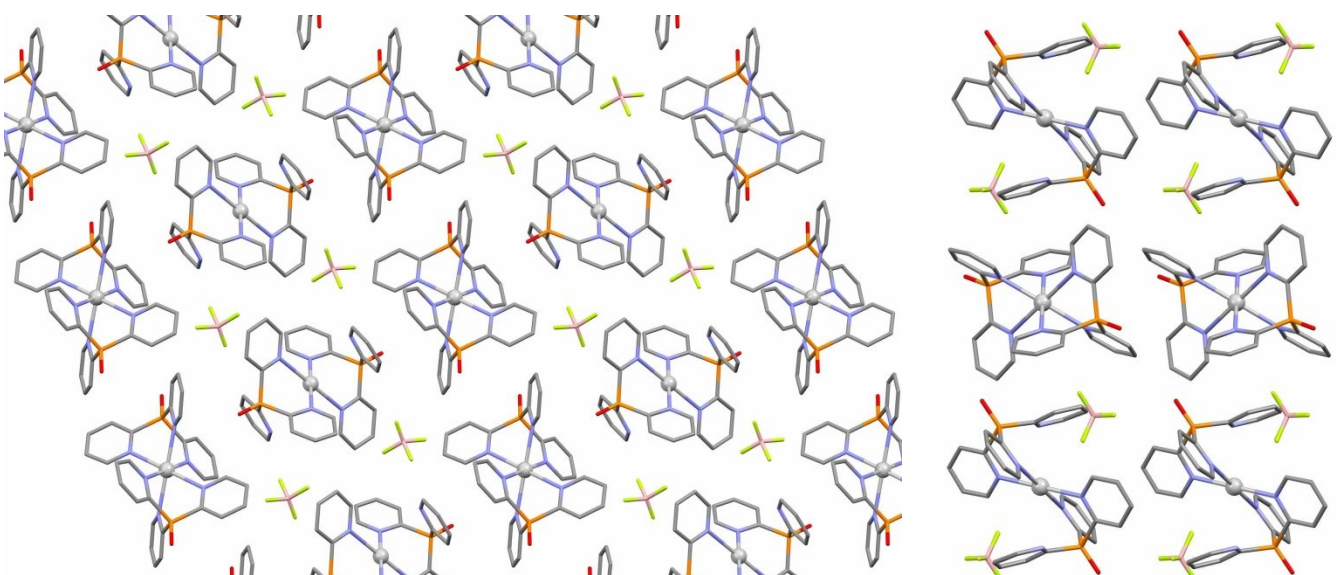


Fig. S6. Perspective view of crystal packing of **3** along *a* (left) and *c* axes (the H atoms are omitted).

§4. TG, DTG and c-DTA curves

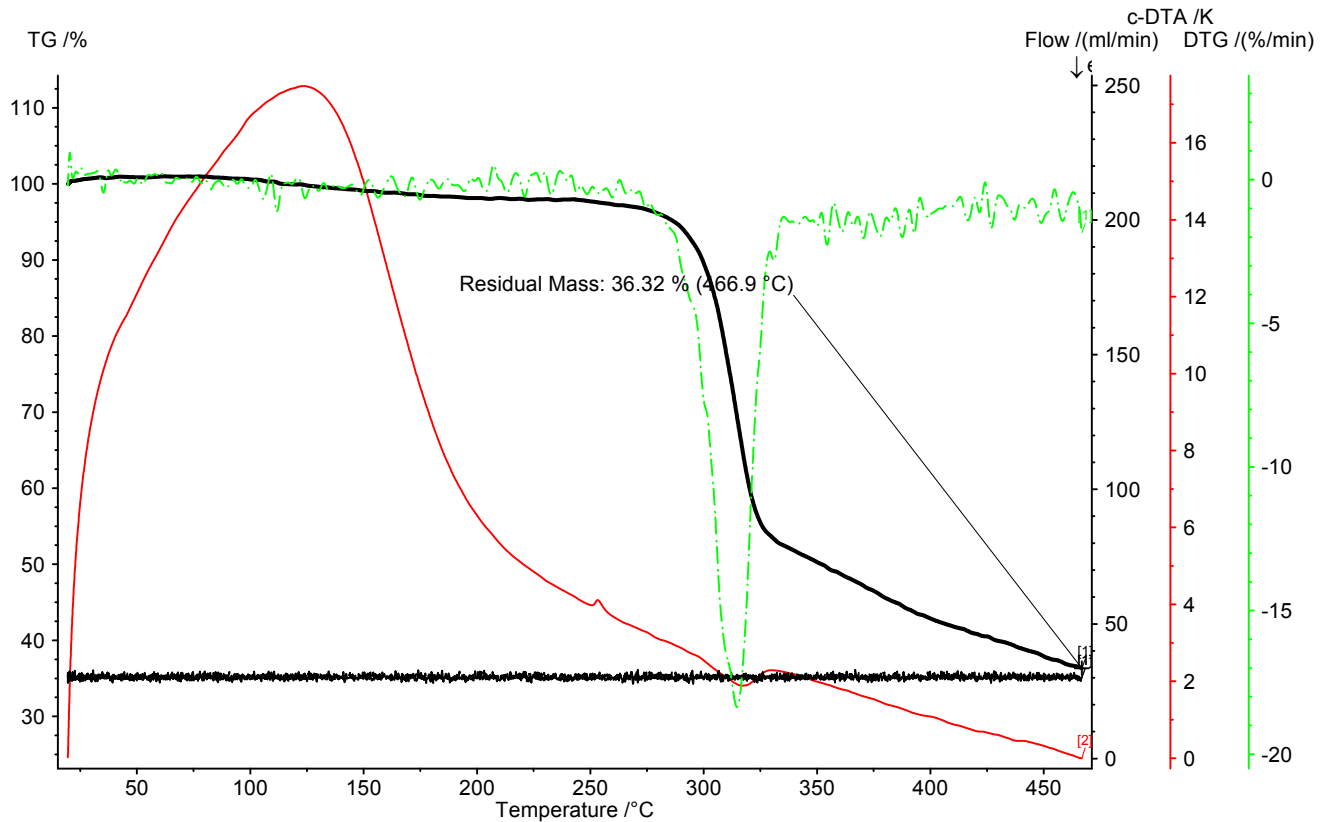


Fig. S7. TG, DTG and c-DTA curves for **1** (He flow, 10 °C/min).

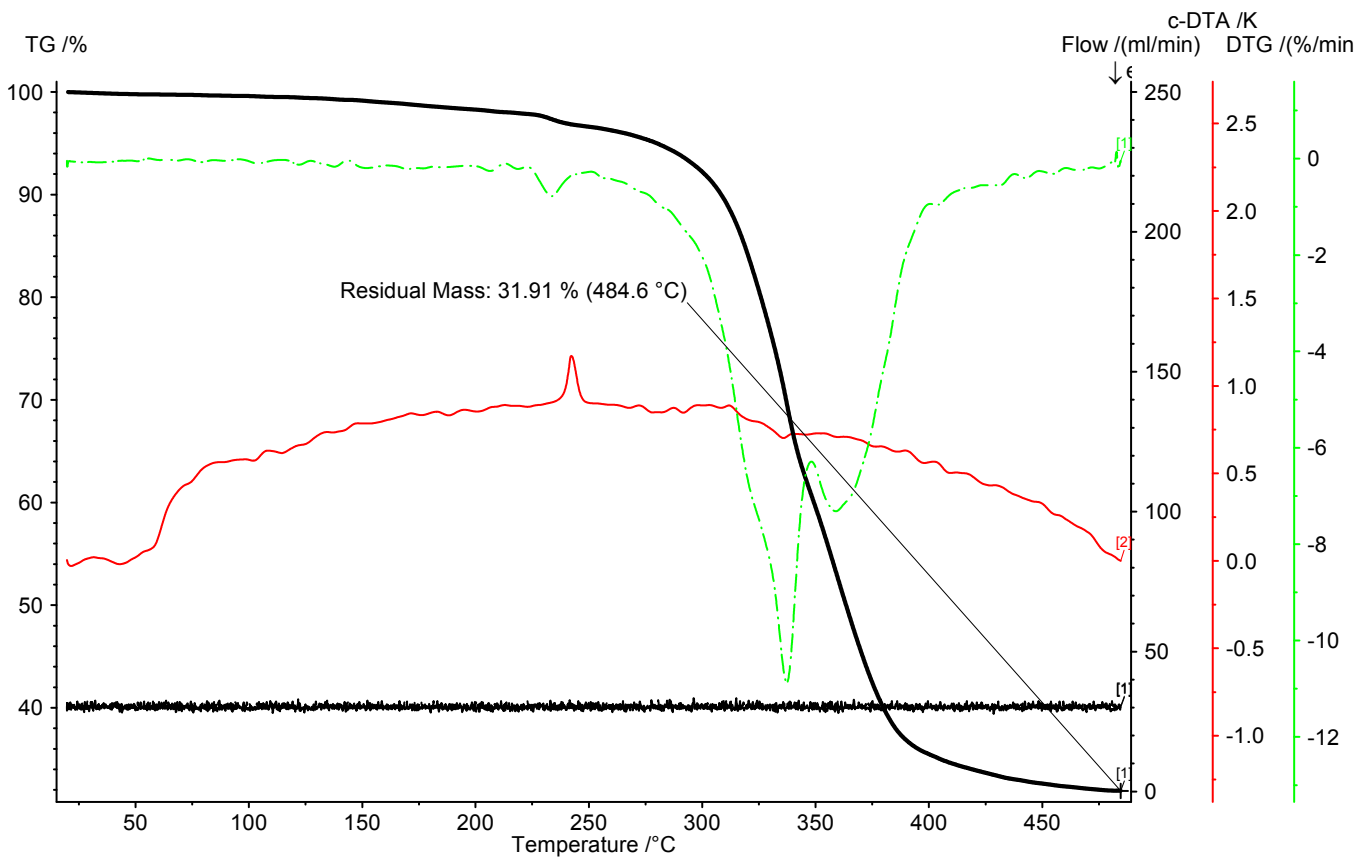


Fig. S8. TG, DTG and c-DTA curves for **2** (He flow, 10 °C/min).

§5. FT-IR spectra

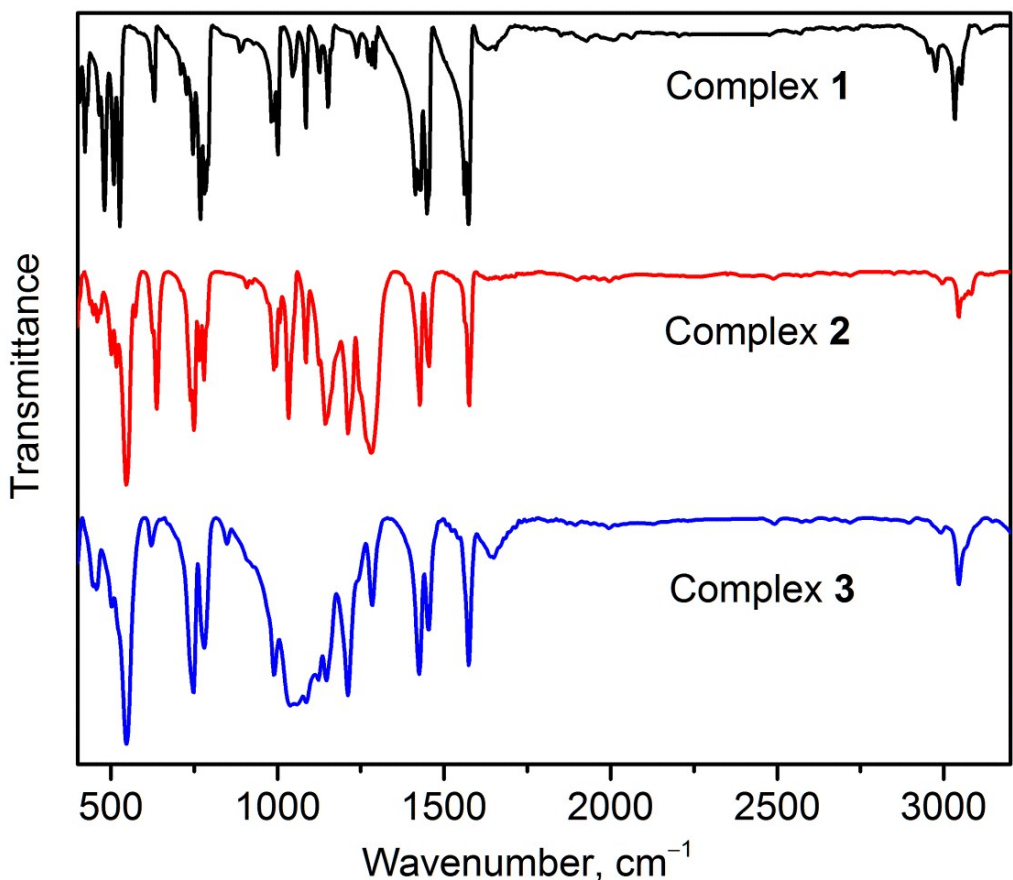


Fig. S9. FT-IR spectra of complexes 1–3.

§6. ESI-MS spectra

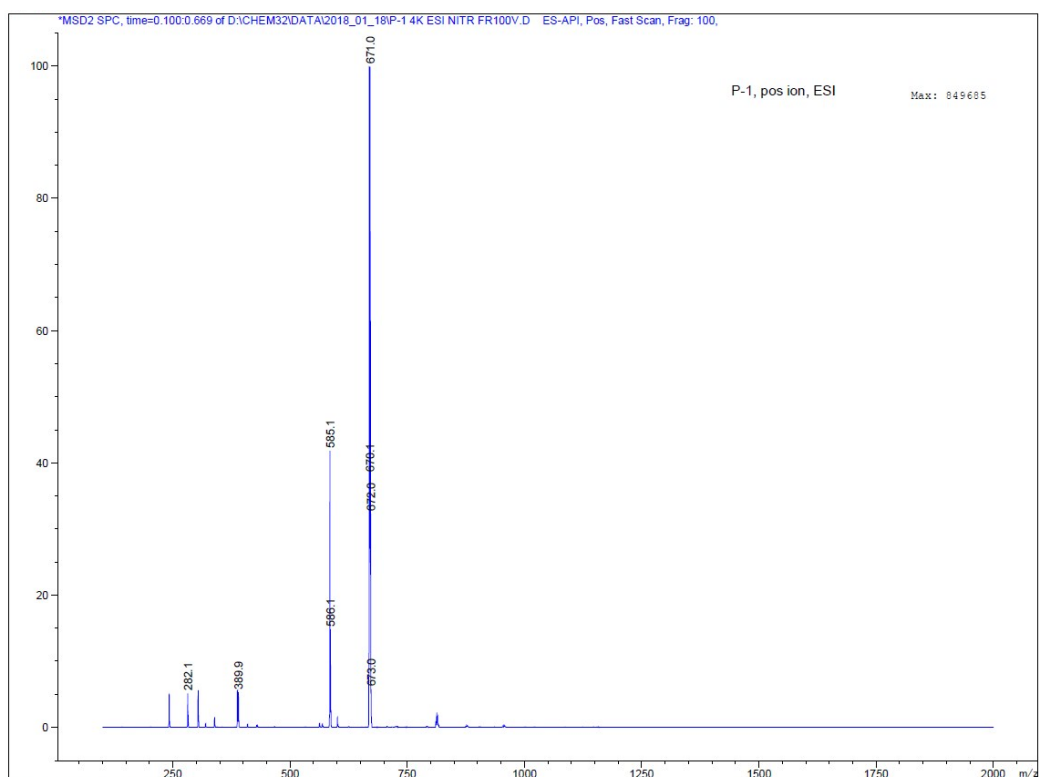


Fig. S10. ESI-Mass spectrum of **1** in the positive-ion mode ionization (MeCN solution).

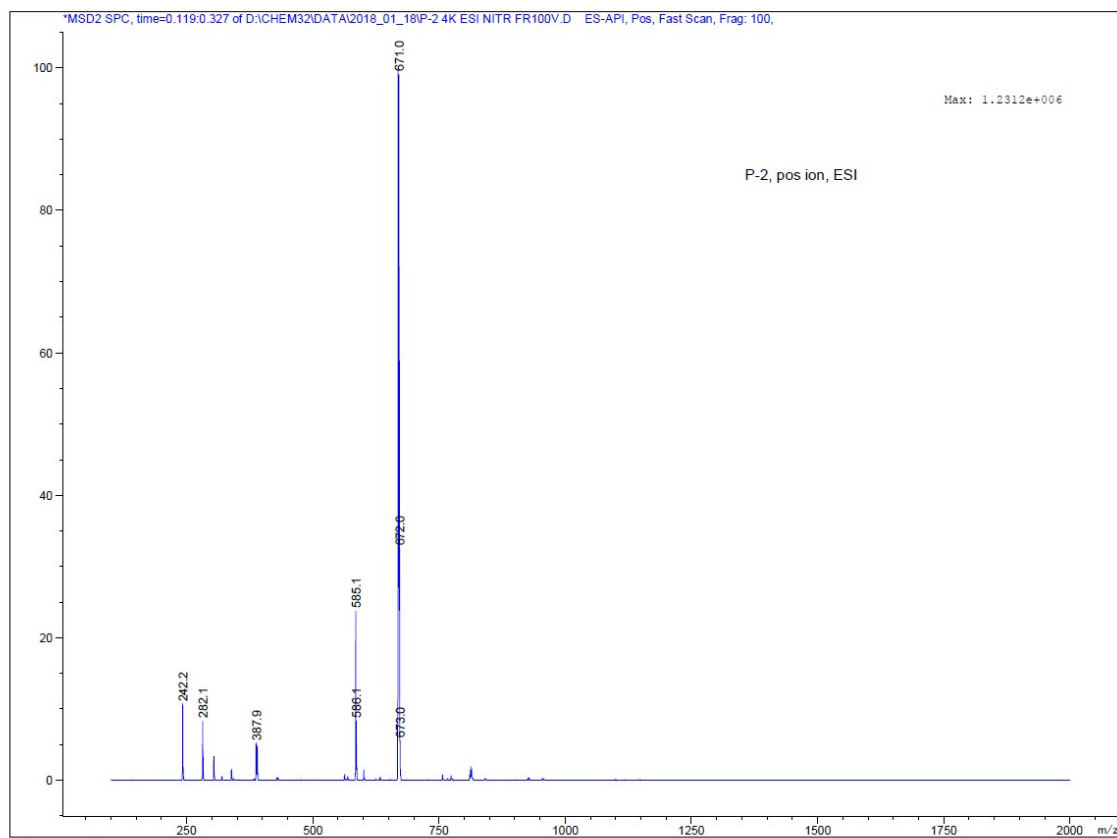


Fig. S11. ESI-Mass spectrum of **2** in the positive-ion mode ionization (MeCN solution).

§7. NMR spectra

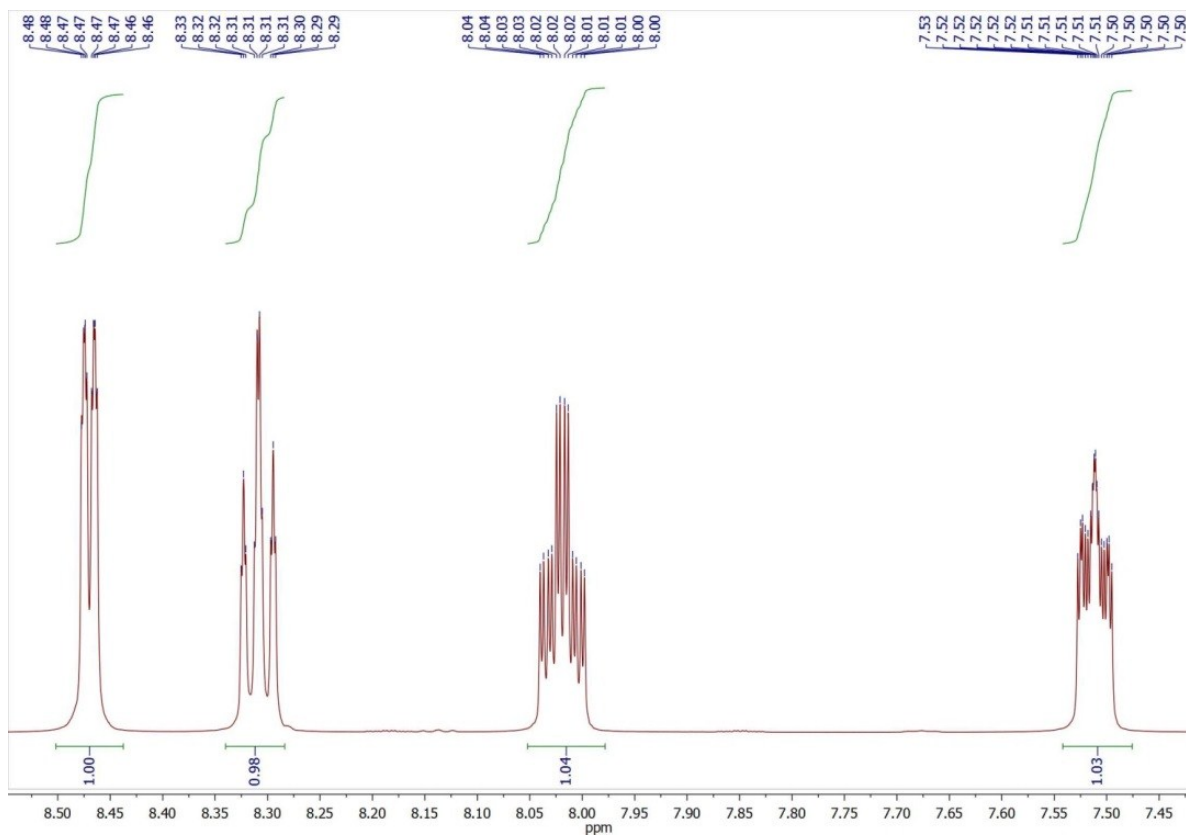


Fig. S12. ^1H NMR spectrum of **1** (CD_3CN , 23 °C).

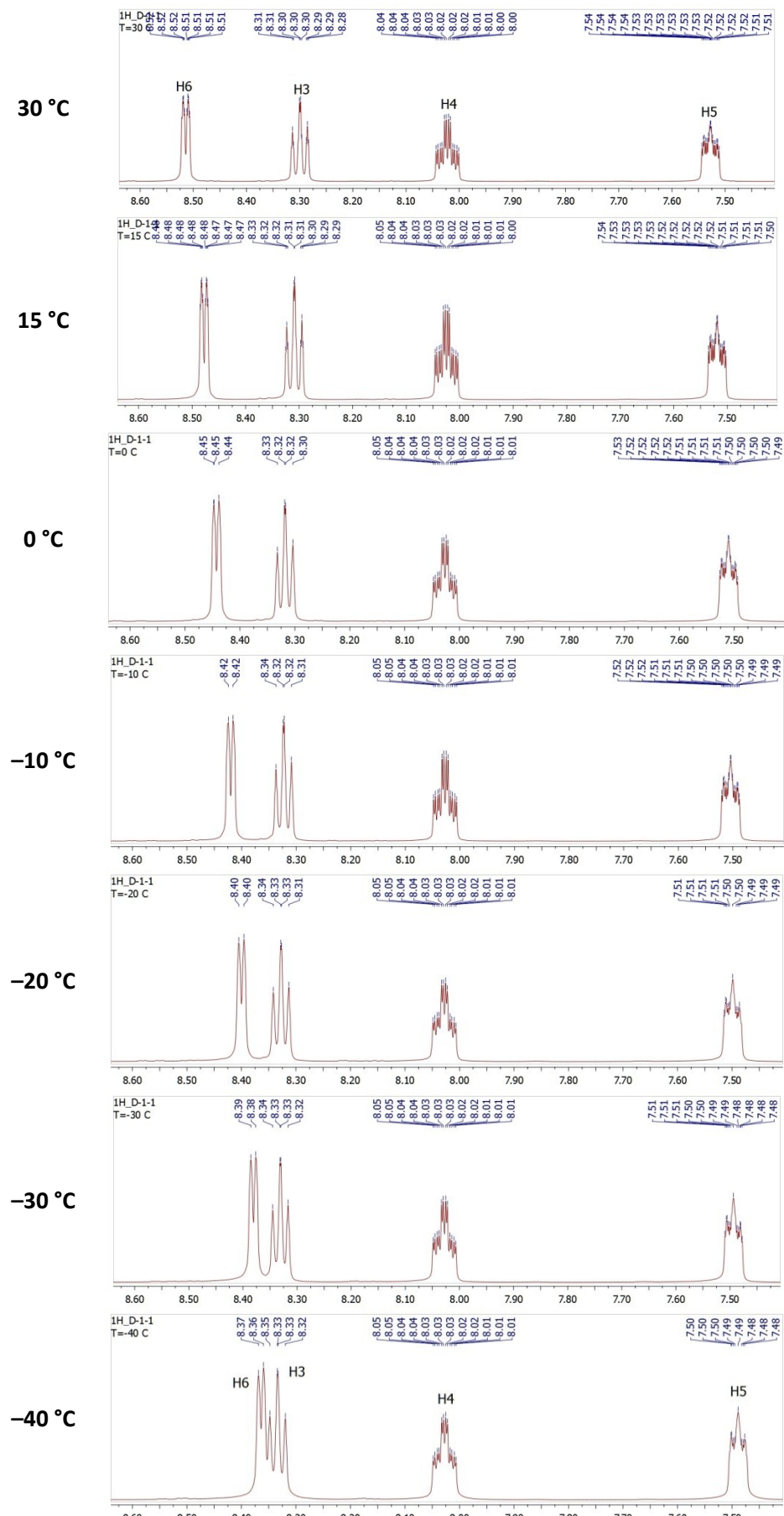


Fig. S13. Variable temperature ¹H NMR spectra of **1** recorded in CD₃CN.

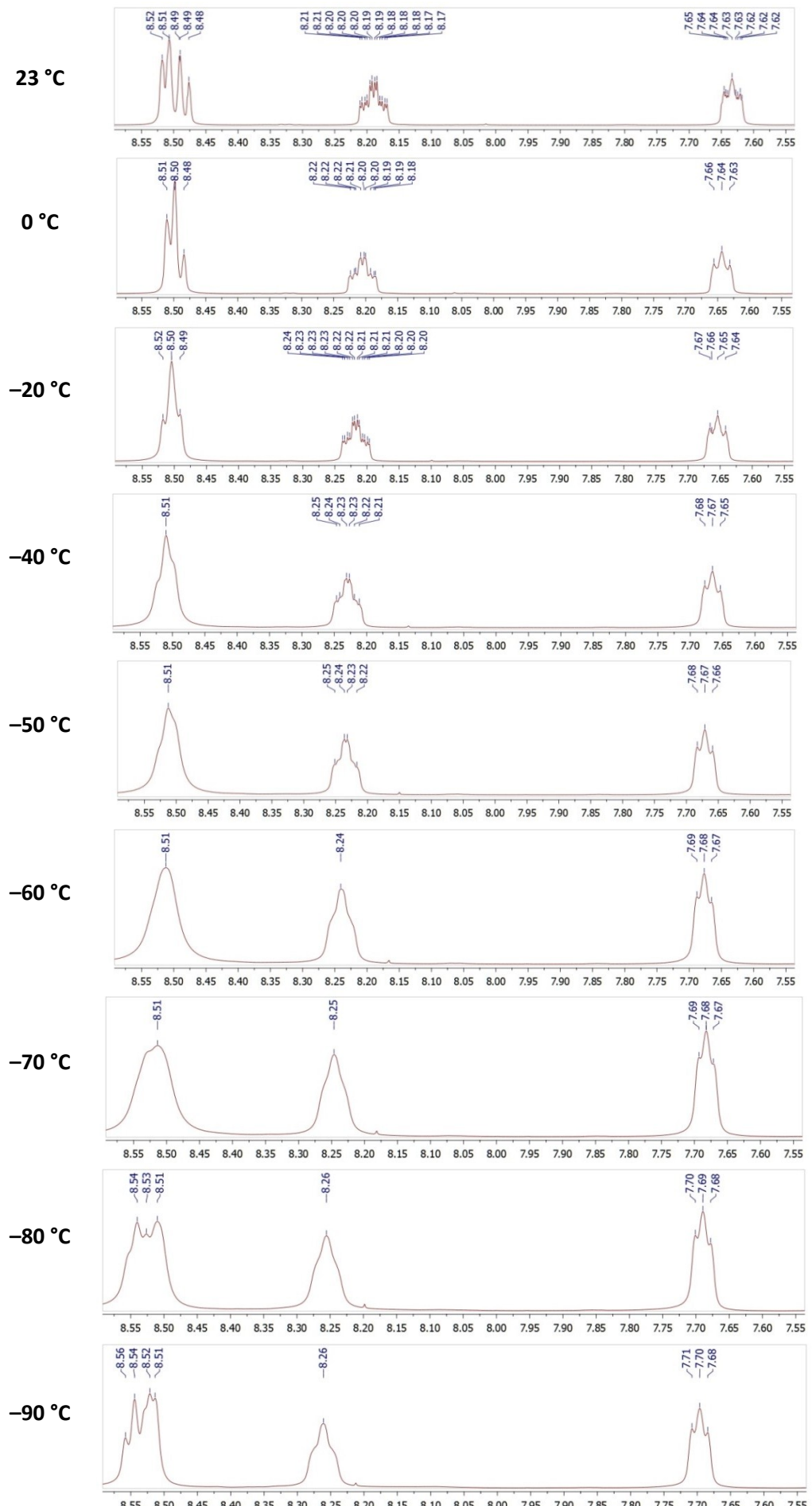


Fig. S14. Variable temperature ¹H NMR spectra of **1** recorded in (CD₃)₂CO.

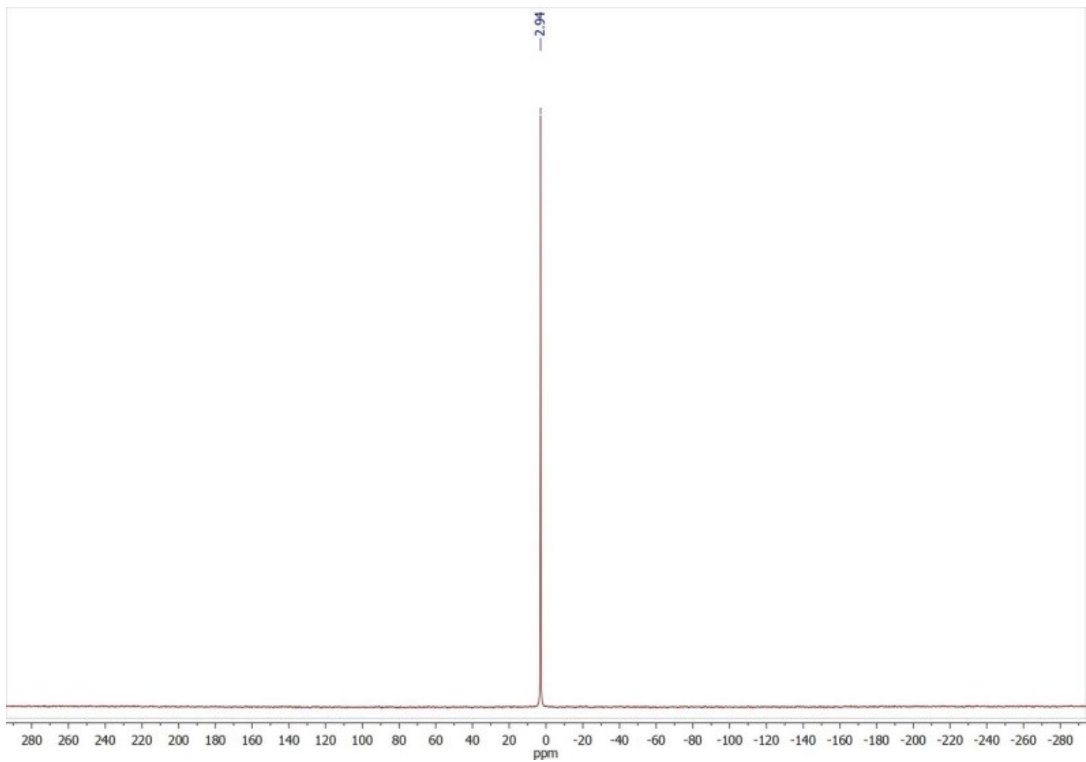


Fig. S15. $^{31}\text{P}\{\text{H}\}$ NMR spectrum of **1** (CD_3CN , 23 °C).

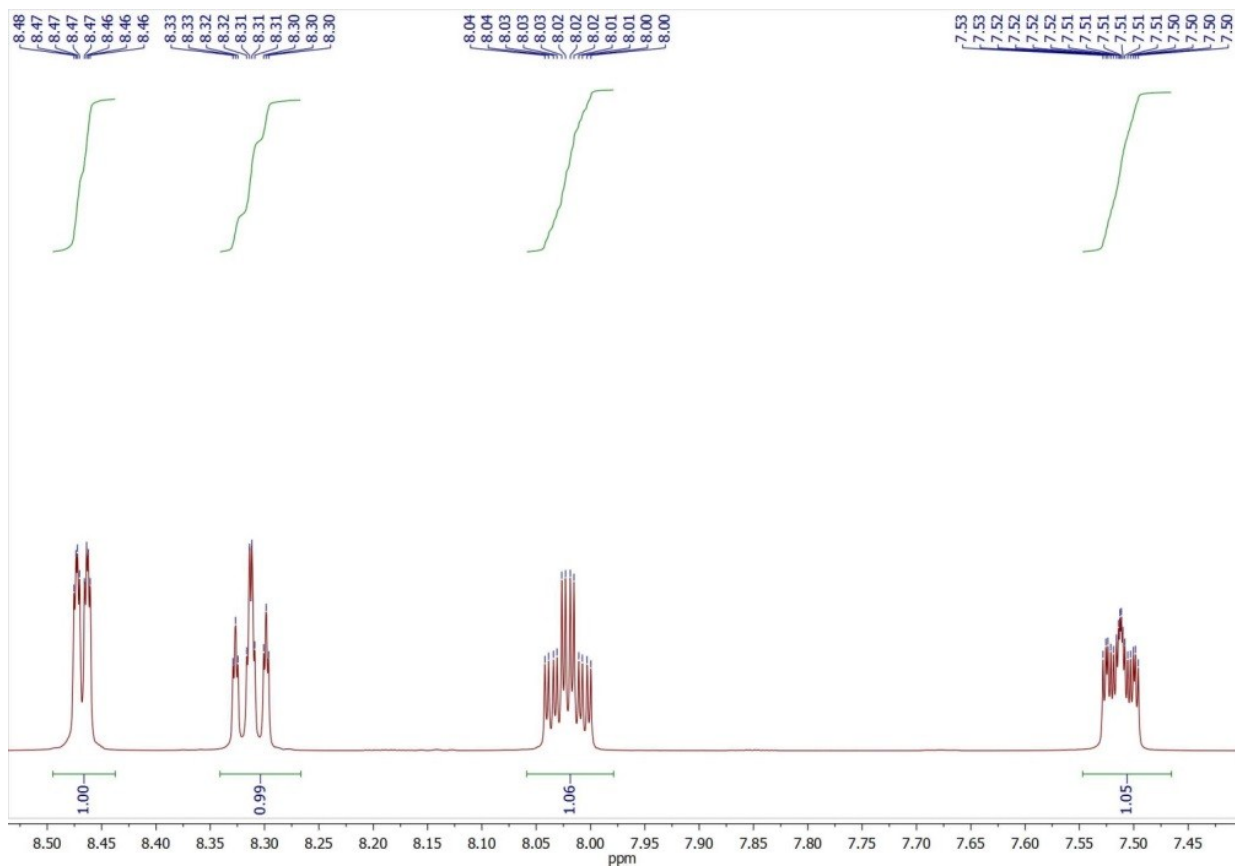


Fig. S16. ^1H NMR spectrum of **2** (CD_3CN , 23 °C).

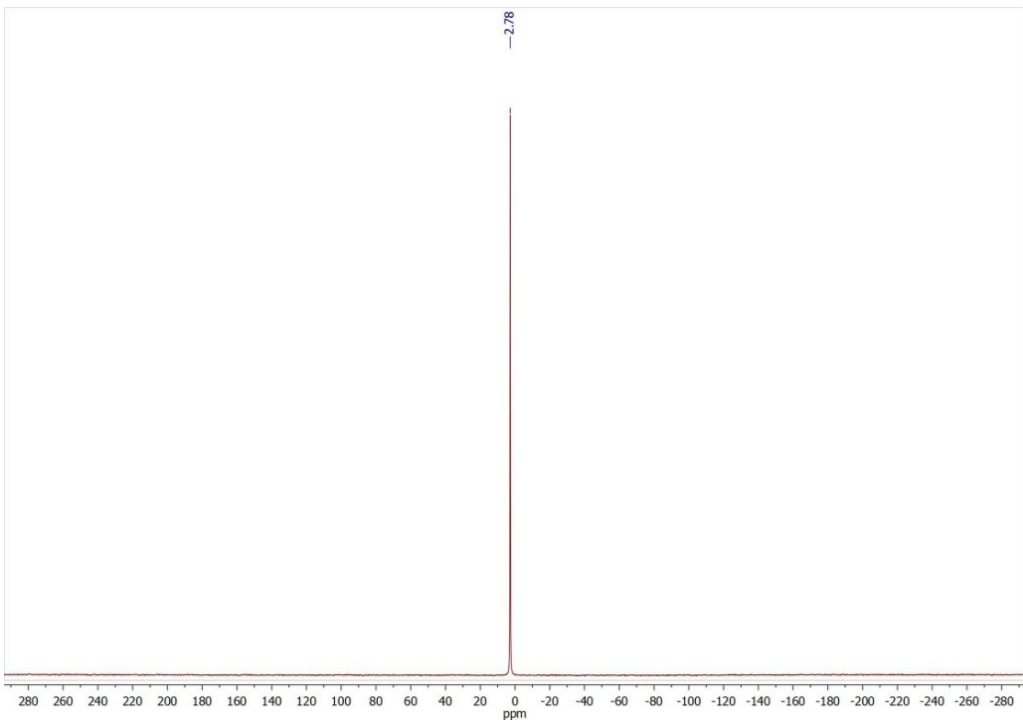


Fig. S17. $^{31}\text{P}\{\text{H}\}$ NMR spectrum of **2** (CD_3CN , 23 °C).

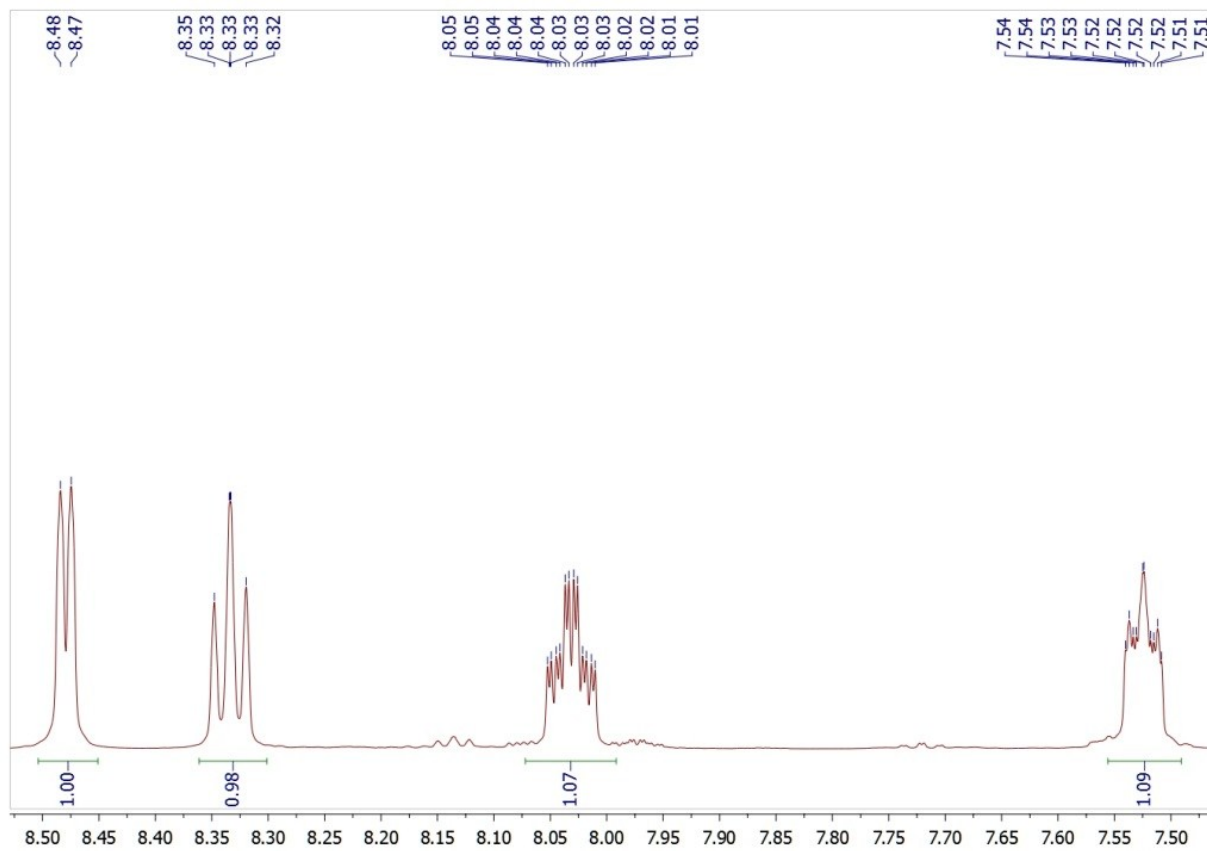


Fig. S18. ^1H NMR spectrum of **3** (CD_3CN , 23 °C).

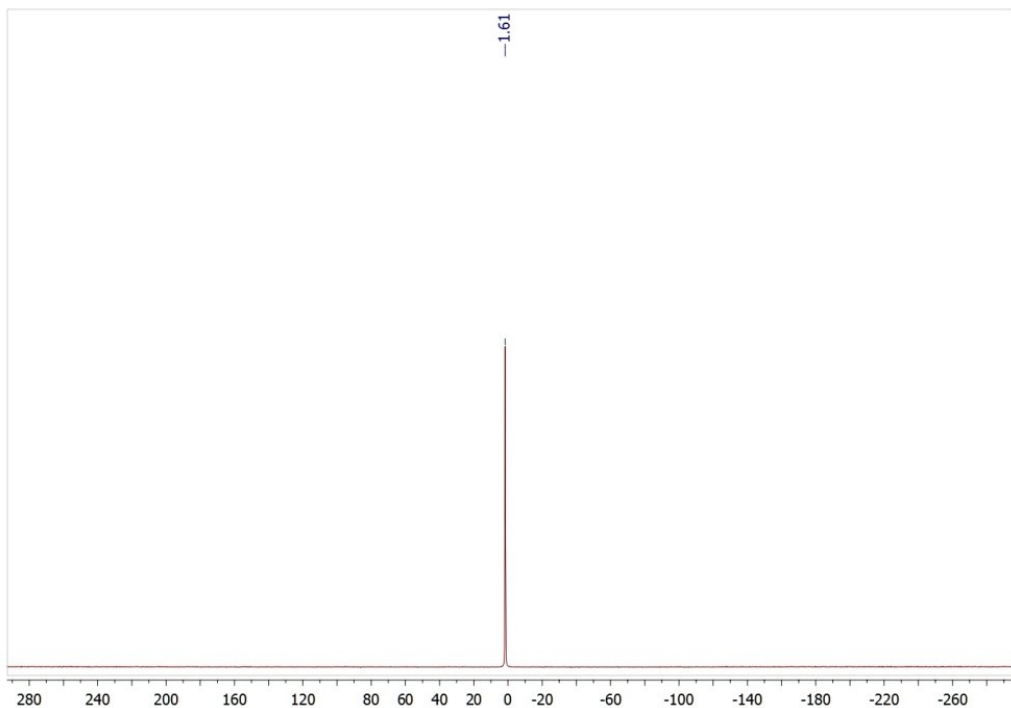


Fig. S19. $^{31}\text{P}\{^1\text{H}\}$ NMR spectrum of **3** (CD_3CN , 23 °C).

§8. Computational details

The geometries of the square-planar, $[\text{Ag}(N,N'\text{-Py}_3\text{PO})_2]^+$, and bis-scorpionate, $[\text{Ag}(N,N',N''\text{-Py}_3\text{PO})_2]^+$, cations, determined from SC-XRD analysis, were used as the initial input for DFT computations. Most of the tested functionals proved unsuitable for localization of the square-planar form as local minimum. However, S12g+PBE+PW92 functional [5–7] (for exchange GGA, correlation GGA and LDA parts, respectively) proved to be applicable for optimization of the square-planar form (fully optimized form). This functional was also used for optimization of the bis-scorpionate form; optimized geometry, however, displays at least one imaginary frequency. So, the hybrid S12h [5] functional was further used for optimization of the bis-scorpionate form. Calculated vibrational spectrum of the latter displays no imaginary frequencies. For estimation of the relative stabilities of square-planar and bis-scorpionate forms, single point calculations of the former were also performed with S12h functional. Geometry of the first triplet (T_1^{SP}) and first singlet (S_1^{SP}) state of the square-planar form was optimized with S12g+PBE+PW92 functional, whereas single point calculations were carried out with S12h density functional. For computation of the structure of square-planar cation of **1** in the solid state, the partial optimization of its S_0 state was performed with S12g+PBE+PW92 functional using frozen X-ray geometry (only H atoms were optimized). The “partially optimized” form, thus obtained, was further utilized for single point calculations of S_0 , S_1 and T_1 states with S12h functional.

All the calculations were performed with all-electron TZP basis set [8] in ADF2017 program suit [9–11]. Scalar relativistic effects were taken into account with Zero Order Regular Approximation (ZORA) [12]. TD-DFT computations of the UV-Vis spectrum were performed for S_0^{SP} state of the fully and partially optimized forms of square-planar $[\text{Ag}(N,N'\text{-Py}_3\text{PO})_2]^+$ cation [13, 14] at S12h/TZP//S12g+PBE+PW92/TZP level of theory. ELF (Electron Localization Function) [15, 16] and QTAIM (Quantum Theory of Atoms In

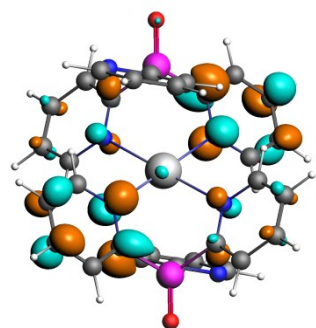
Molecules) [17] analysis were performed in Dgrid4.6 [18] program with 0.05 a.u. (0.026 Å) mesh step. Cartesian coordinates for all computed structures are given below.

Table S2. Wavelengths, oscillator strengths, few highest contributions of single orbital transitions, contributions of atomic orbitals of ligands atoms and Ag⁺ cation to occupied and unoccupied MOs for selected excitations of the fully optimized square-planar [Ag(*N,N'*-Py₃PO)₂]⁺ cation.

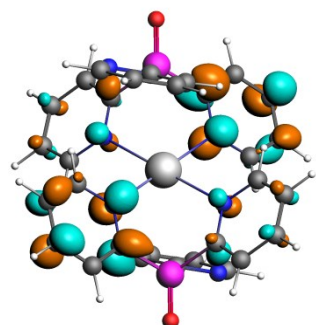
Wavelength, nm	Oscillator strength (<i>f</i>), a.u.	Contributions of single orbital transitions	Composition of occupied MO		Composition of unoccupied MO	
			Ligands	Ag ⁺	Ligands	Ag ⁺
237	0.11	24% HOMO-6 → LUMO	100%	0%	100%	0%
		15% HOMO-1 → LUMO+5	90%	10%	100%	0%
		11% HOMO-7 → LUMO+1	100%	0%	100%	0%
		5% HOMO-1 → LUMO+8	90%	10%	100%	0%
		4% HOMO-2 → LUMO+9	100%	0%	100%	0%
238	0.09	21% HOMO-6 → LUMO	100%	0%	100%	0%
		15% HOMO-1 → LUMO+5	90%	10%	100%	0%
		14% HOMO-5 → LUMO+1	100%	0%	100%	0%
		10% HOMO-4 → LUMO+1	100%	0%	100%	0%
		5% HOMO-8 → LUMO	88%	12%	100%	0%
239	0.07	13% HOMO-1 → LUMO+2	90%	10%	99%	1%
		9% HOMO-3 → LUMO+2	90%	10%	99%	1%
		8% HOMO-1 → LUMO+3	90%	10%	100%	0%
		8% HOMO-3 → LUMO+3	90%	10%	100%	0%
		6% HOMO-4 → LUMO+3	100%	0%	100%	0%
367	0.01	98% HOMO → LUMO	56%	44%	100%	0%

Table S3. Experimental emission maxima at 300 K and 77 K and calculated energy difference between S₀ and T₁ (or S₁) states for fully optimized (FO) and partially optimized (PO) square-planar [Ag(*N,N'*-Py₃PO)₂]⁺ cation. All values are given in nm.

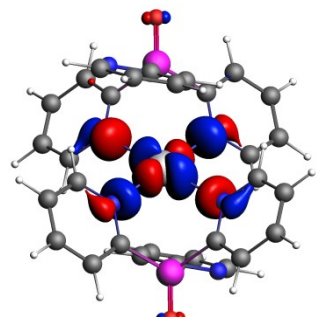
	ΔE(T ₁ –S ₀)	ΔE(S ₁ –S ₀)	λ ^{em} <i>max</i> at 300K	λ ^{em} <i>max</i> at 77K
[Ag(<i>N,N'</i> -Py ₃ PO) ₂] ⁺ (FO)	535	525		
[Ag(<i>N,N'</i> -Py ₃ PO) ₂] ⁺ (PO)	382	376		
Complex 1			580	620
Complex 2			590	620



LUMO+1



LUMO



HOMO

Fig. S20. Frontier MOs for S₀ state of partially optimized form of square-planar [Ag(N,N'-Py₃PO)₂]⁺ cation.

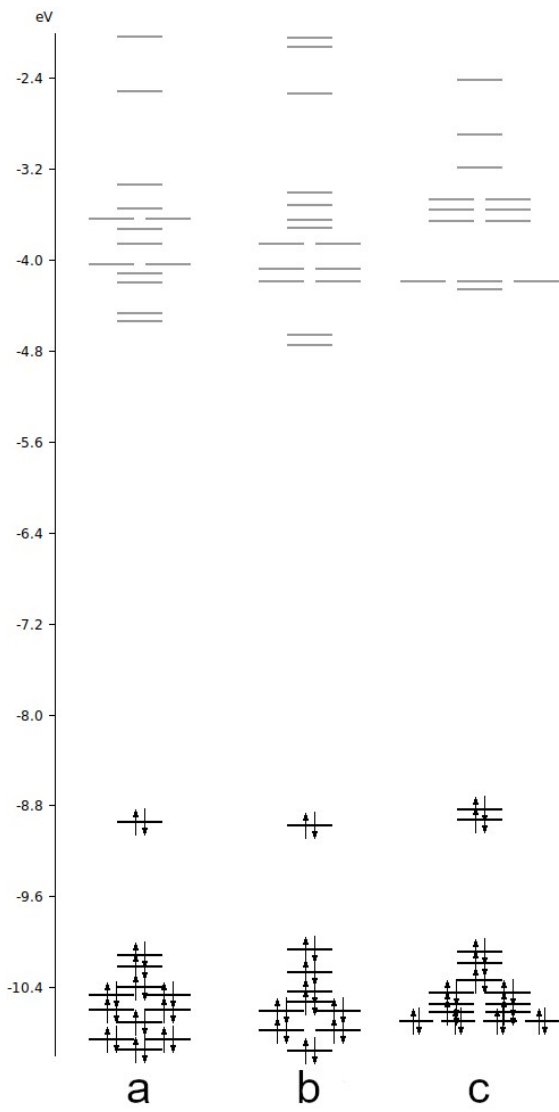


Fig. S21. MO diagram for S_0 states of fully optimized square-planar $[\text{Ag}(N,N'\text{-Py}_3\text{PO})_2]^+$ cation (**a**), partially optimized (non-hydrogen atoms were fixed at X-ray geometry) square-planar $[\text{Ag}(N,N'\text{-Py}_3\text{PO})_2]^+$ cation (**b**) and fully optimized bis-scorpionate $[\text{Ag}(N,N',N''\text{-Py}_3\text{PO})_2]^+$ cation (**c**).

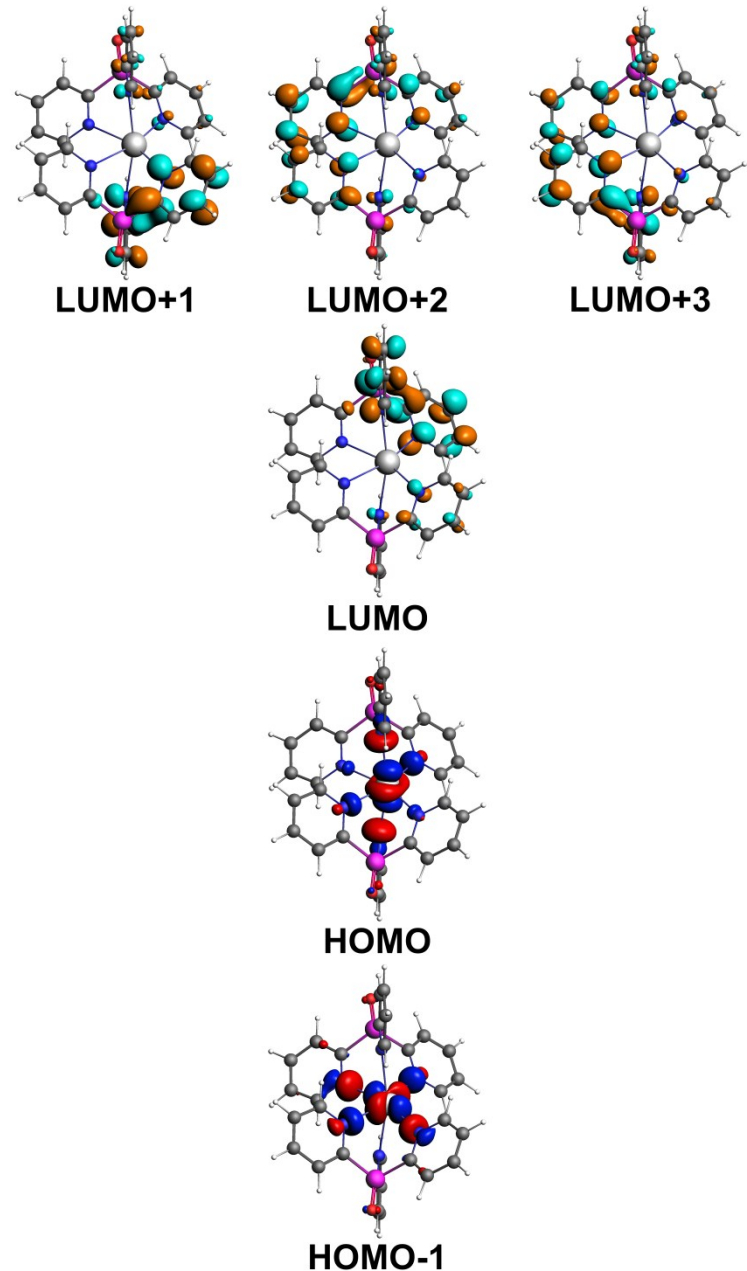


Fig S22. Frontier MOs for S_0 state of bis-scorpionate $[\text{Ag}(\text{N},\text{N}',\text{N}''-\text{Py}_3\text{PO})_2]^+$ cation.

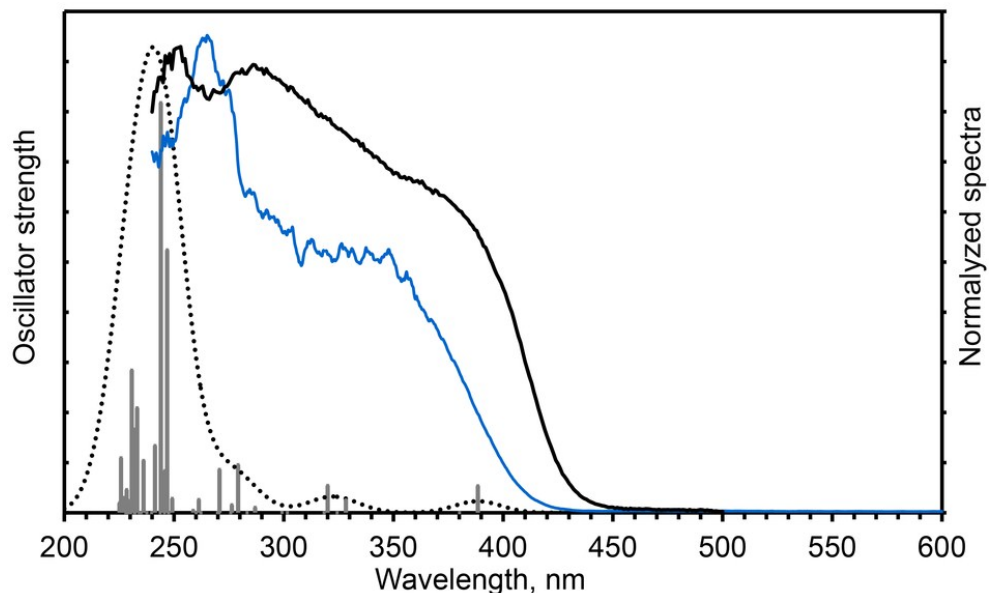


Fig S23. The solid-state normalized spectra for complex **1** at 298 K: UV-Vis absorption (blue), luminescence excitation ($\lambda_{\text{reg}} = 580 \text{ nm}$, black) spectra. Vertical bars display the positions and oscillator strengths (f) of the electronic transitions computed at the S12h/TZP//S12g/TZP level for partially optimized square-planar $[\text{Ag}(N,N'\text{-Py}_3\text{PO})_2]^+$ cation.

Table S4. Parameters in QTAIM bond critical points for singlet (S_0^{SP}) and triplet (T_1^{SP}) states of the square-planar $[\text{Ag}(N,N'\text{-Py}_3\text{PO})_2]^+$ cation. All values are in atomic units.

Bond or contact	$\rho(r)^a$	$\nabla^2\rho(r)^b$	$ V(r) /G(r)^c$	H_b^d
S_0^{SP}				
Ag–N1	0.049	0.191	1.096	-0.005
Ag–N2	0.044	0.167	1.082	-0.004
Ag···C _{Py}	0.014	0.043	0.953	0.0003
T_1^{SP}				
Ag–N1	0.068	0.243	1.158	-0.011
Ag–N2	0.069	0.247	1.159	-0.012
Ag···N3	0.030	0.107	1.029	-0.001

^a Electron density;

^b Laplacian of electron density;

^c $V(r)$ – potential energy density, and $G(r)$ – kinetic energy density;

^d Total energy density ($V+G$).

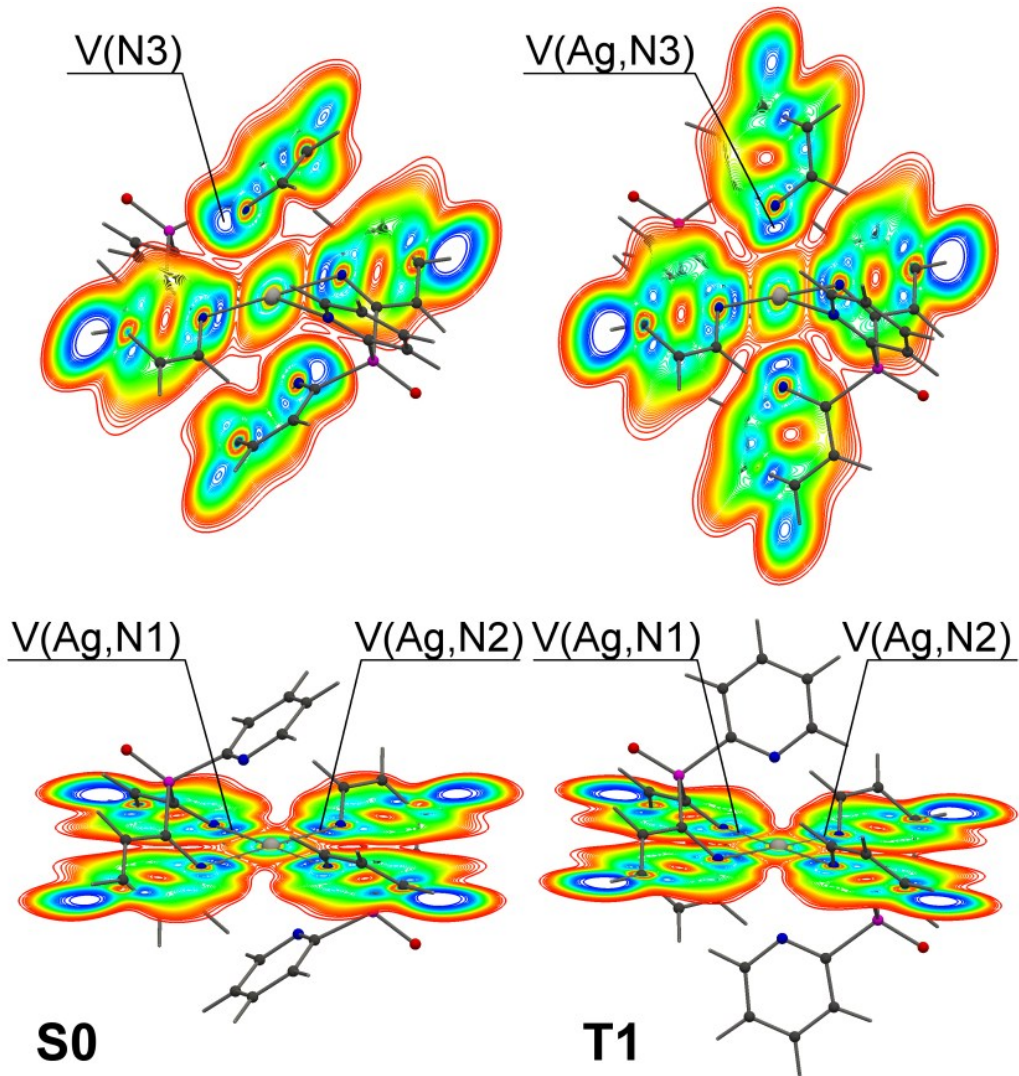


Fig. S24. ELF distribution in Ag–N1–N3 (top) and Ag–N1–N2 planes (bottom) for S_0^{SP} and T_1^{SP} states of the $[\text{Ag}(\text{Py}_3\text{PO})_2]^+$ cation.

Cartesian coordinates (\AA) for S_0 state of fully optimized square-planar $[\text{Ag}(N,N'\text{-Py}_3\text{PO})_2]^+$ cation.

Ag	0.000661000	-0.027102000	-0.027122000
P	3.257968000	-0.650127000	0.735509000
P	-3.257024000	0.657835000	-0.724237000
O	4.657866000	-0.957282000	1.148072000
O	-4.657416000	0.982698000	-1.121175000
N	1.380746000	-2.582235000	1.207377000
N	1.614680000	1.555061000	0.806906000
N	1.738697000	-0.843983000	-1.551937000
N	-1.397756000	2.590795000	-1.227207000
N	-1.653989000	-1.583089000	-0.793015000
N	-1.693759000	0.867467000	1.527924000
C	0.277475000	-2.924114000	3.323791000
C	0.556719000	-3.272387000	2.003801000
C	0.897505000	-1.801455000	3.861898000
C	1.359807000	2.862270000	0.947341000
C	1.536108000	-1.205054000	-2.823766000
C	1.766236000	-1.073885000	3.057571000
C	1.966582000	-1.496858000	1.739872000
C	2.361230000	3.801959000	1.178056000

C	2.504212000	-1.844831000	-3.594055000
C	2.891928000	1.146913000	0.893049000
C	2.936021000	-1.116548000	-1.011055000
C	3.681656000	3.372093000	1.263693000
C	3.742965000	-2.117472000	-3.023901000
C	3.957315000	2.014481000	1.120588000
C	3.969349000	-1.741983000	-1.702713000
C	-0.280942000	2.905776000	-3.340142000
C	-0.575712000	3.275861000	-2.029250000
C	-0.883595000	1.766149000	-3.861811000
C	-1.427966000	-2.895671000	-0.934483000
C	-1.462817000	1.236462000	2.792331000
C	-1.749301000	1.042280000	-3.050505000
C	-1.964801000	1.487278000	-1.742324000
C	-2.417115000	1.872955000	3.582500000
C	-2.448775000	-3.813089000	-1.169210000
C	-2.905830000	1.127336000	1.015308000
C	-2.922020000	-1.146609000	-0.881932000
C	-3.671992000	2.131744000	3.041742000
C	-3.759239000	-3.354516000	-1.257478000
C	-3.927682000	1.747830000	1.728198000
C	-4.004907000	-1.991357000	-1.113093000
H	0.091306000	-4.154953000	1.560746000
H	0.310482000	3.150848000	0.870792000
H	0.400387000	3.508143000	-3.938280000
H	0.552743000	-0.974154000	-3.234969000
H	0.714469000	-1.502419000	4.893147000
H	2.101925000	4.852819000	1.294282000
H	2.283115000	-2.123539000	-4.622754000
H	2.287196000	-0.197987000	3.442032000
H	4.487028000	4.082344000	1.445545000
H	4.522536000	-2.617537000	-3.596843000
H	4.914598000	-1.925953000	-1.195160000
H	4.966246000	1.611761000	1.193184000
H	-0.125140000	4.172361000	-1.598975000
H	-0.385869000	-3.208284000	-0.856384000
H	-0.406253000	-3.529607000	3.915986000
H	-0.467389000	1.016474000	3.179742000
H	-0.689331000	1.450747000	-4.886146000
H	-2.173157000	2.160181000	4.603699000
H	-2.211599000	-4.869077000	-1.286072000
H	-2.255511000	0.152579000	-3.422630000
H	-4.441126000	2.628793000	3.631160000
H	-4.579573000	-4.046571000	-1.442373000
H	-4.885627000	1.923741000	1.242009000
H	-5.004544000	-1.566309000	-1.186854000

Cartesian coordinates (Å) for T₁ state of fully optimized square-planar [Ag(N,N'-Py₃PO)₂]⁺ cation.

Ag	0.000000000	0.000000000	0.000000000
P	3.243121880	-0.617687030	1.083505840
P	-3.243121880	0.617687030	-1.083505840
O	4.675216650	-0.812501810	1.450081860
O	-4.675216650	0.812501810	-1.450081860
N	0.819081080	-1.587749300	1.967584930
N	1.496319360	1.510525540	0.748920310
N	1.671414510	-0.912975610	-1.194673450
N	-0.819081080	1.587749300	-1.967584930
N	-1.496319360	-1.510525540	-0.748920310
N	-1.671414510	0.912975610	1.194673450

C	0.037346030	-2.233445870	2.840527520
C	0.525847400	-2.844226620	3.992996660
C	1.193716150	2.822741840	0.730680820
C	1.498349220	-1.199892840	-2.498022280
C	1.891153670	-2.781141940	4.255799790
C	2.102715050	3.799412840	1.098054100
C	2.133084880	-1.530229860	2.234209490
C	2.509580760	-1.726381180	-3.283656630
C	2.718182730	-2.108558560	3.360395800
C	2.743717450	1.134720180	1.123477240
C	2.887005470	-1.125218090	-0.634804080
C	3.391633360	3.415756250	1.494297710
C	3.714164260	2.065813740	1.499119910
C	3.765279680	-1.959541510	-2.707674250
C	3.955155920	-1.643607170	-1.369264080
C	-0.037346030	2.233445870	-2.840527520
C	-0.525847400	2.844226620	-3.992996660
C	-1.193716150	-2.822741840	-0.730680820
C	-1.498349220	1.199892840	2.498022280
C	-1.891153670	2.781141940	-4.255799790
C	-2.102715050	-3.799412840	-1.098054100
C	-2.133084880	1.530229860	-2.234209490
C	-2.509580760	1.726381180	3.283656630
C	-2.718182730	2.108558560	-3.360395800
C	-2.743717450	-1.134720180	-1.123477240
C	-2.887005470	1.125218090	0.634804080
C	-3.391633360	-3.415756250	-1.494297710
C	-3.714164260	-2.065813740	-1.499119910
C	-3.765279680	1.959541510	2.707674250
C	-3.955155920	1.643607170	1.369264080
H	0.155479800	3.361044920	-4.666503580
H	0.185059850	3.077651820	0.409206690
H	0.509311400	-0.996627160	-2.906789490
H	1.026982170	2.262324790	-2.598215620
H	1.804147500	4.845210530	1.071820360
H	2.308978420	-3.251301490	5.144906690
H	2.314266090	-1.948485630	-4.330588240
H	3.793591350	-2.027902290	3.506958890
H	4.128669270	4.160161740	1.789522550
H	4.580477270	-2.374991340	-3.297056310
H	4.699869590	1.702458130	1.784894560
H	4.911320710	-1.783120260	-0.867772170
H	-0.155479800	-3.361044920	4.666503580
H	-0.185059850	-3.077651820	-0.409206690
H	-0.509311400	0.996627160	2.906789490
H	-1.026982170	-2.262324790	2.598215620
H	-1.804147500	-4.845210530	-1.071820360
H	-2.308978420	3.251301490	-5.144906690
H	-2.314266090	1.948485630	4.330588240
H	-3.793591350	2.027902290	-3.506958890
H	-4.128669270	-4.160161740	-1.789522550
H	-4.580477270	2.374991340	3.297056310
H	-4.699869590	-1.702458130	-1.784894560
H	-4.911320710	1.783120260	0.867772170

Cartesian coordinates (Å) for S₁ state of fully optimized square-planar [Ag(*N,N'*-Py₃PO)₂]⁺ cation.

Ag	-0.000004000	-0.000048000	-0.000003000
P	3.243885000	-0.615668000	1.086681000
P	-3.243896000	0.615639000	-1.086656000

O	4.676283000	-0.808415000	1.453261000
O	-4.676296000	0.808410000	-1.453217000
N	0.819051000	-1.577772000	1.977266000
N	1.495002000	1.510265000	0.745285000
N	1.672658000	-0.919756000	-1.190449000
N	-0.819057000	1.577675000	-1.977291000
N	-1.495033000	-1.510324000	-0.745297000
N	-1.672647000	0.919676000	1.190459000
C	0.038574000	-2.226265000	2.849237000
C	0.530259000	-2.850613000	3.993076000
C	1.191604000	2.821930000	0.724748000
C	1.499181000	-1.211524000	-2.492209000
C	1.897611000	-2.799188000	4.247643000
C	2.098111000	3.800213000	1.094383000
C	2.135097000	-1.531236000	2.236163000
C	2.511147000	-1.737395000	-3.277734000
C	2.723397000	-2.123715000	3.353264000
C	2.741646000	1.135630000	1.124517000
C	2.889527000	-1.125971000	-0.631322000
C	3.386207000	3.417831000	1.495274000
C	3.709833000	2.068244000	1.502690000
C	3.768598000	-1.963163000	-2.702578000
C	3.958930000	-1.642402000	-1.365401000
C	-0.038581000	2.226173000	-2.849260000
C	-0.530278000	2.850578000	-3.993064000
C	-1.191644000	-2.821992000	-0.724803000
C	-1.499141000	1.211478000	2.492208000
C	-1.897636000	2.799194000	-4.247603000
C	-2.098170000	-3.800258000	-1.094432000
C	-2.135109000	1.531185000	-2.236158000
C	-2.511056000	1.737475000	3.277714000
C	-2.723420000	2.123711000	-3.353228000
C	-2.741683000	-1.135670000	-1.124489000
C	-2.889499000	1.125975000	0.631327000
C	-3.386282000	-3.417857000	-1.495249000
C	-3.709894000	-2.068266000	-1.502635000
C	-3.768480000	1.963359000	2.702546000
C	-3.958845000	1.642565000	1.365382000
H	0.150234000	3.368658000	-4.666394000
H	0.183927000	3.075796000	0.399292000
H	0.508943000	-1.013064000	-2.900476000
H	1.027453000	2.245850000	-2.613621000
H	1.798651000	4.845671000	1.065848000
H	2.315039000	-1.964389000	-4.323451000
H	2.317786000	-3.280158000	5.129879000
H	3.800166000	-2.051009000	3.493908000
H	4.121762000	4.163119000	1.792004000
H	4.584808000	-2.377109000	-3.291647000
H	4.694966000	1.706165000	1.792059000
H	4.916127000	-1.776902000	-0.864488000
H	-0.150256000	-3.368686000	4.666409000
H	-0.183957000	-3.075872000	-0.399386000
H	-0.508920000	1.012941000	2.900482000
H	-1.027455000	-2.245978000	2.613573000
H	-1.798717000	-4.845718000	-1.065936000
H	-2.314927000	1.964486000	4.323424000
H	-2.317818000	3.280203000	-5.129815000
H	-3.800193000	2.051036000	-3.493851000
H	-4.121858000	-4.163133000	-1.791958000
H	-4.584648000	2.377418000	3.291597000

H	-4.695034000	-1.706173000	-1.791962000
H	-4.916028000	1.777139000	0.864464000

Cartesian coordinates (Å) for S₀ state of partially optimized square-planar [Ag(N,N'-Py₃PO)₂]⁺ cation.

Ag	0.000000000	0.000000000	0.000000000
P	3.322744740	-0.091420730	0.887544340
P	-3.322744740	0.091420730	-0.887544340
O	4.702069530	-0.152450600	1.413883510
O	-4.702069530	0.152450600	-1.413883510
N	1.328439910	1.741948180	0.671802910
N	1.967579010	-0.821599270	-1.328761360
N	2.326762100	-2.471491080	1.327714560
N	-1.328439910	-1.741948180	-0.671802910
N	-1.967579010	0.821599270	1.328761360
N	-2.326762100	2.471491080	-1.327714560
C	0.456516000	-1.783399260	3.272641360
C	0.626961980	-3.093805160	2.878951380
C	0.834190060	2.991885360	0.676404470
C	1.240041550	-0.803935760	2.675256850
C	1.564335440	-3.396972340	1.913391920
C	1.618323170	4.103786190	0.914489430
C	1.868346730	-1.216292260	-2.605147660
C	2.140770360	-1.197259280	1.707977060
C	2.639399700	1.585826550	0.951155610
C	2.963785450	3.930975720	1.179386010
C	2.968320180	-1.356382960	-3.431261210
C	3.199431440	-0.590837530	-0.851522000
C	3.482119880	2.646754320	1.230035310
C	4.222305040	-1.088017880	-2.929011320
C	4.352783620	-0.701161050	-1.611481730
C	-0.456516000	1.783399260	-3.272641360
C	-0.626961980	3.093805160	-2.878951380
C	-0.834190060	-2.991885360	-0.676404470
C	-1.240041550	0.803935760	-2.675256850
C	-1.564335440	3.396972340	-1.913391920
C	-1.618323170	-4.103786190	-0.914489430
C	-1.868346730	1.216292260	2.605147660
C	-2.140770360	1.197259280	-1.707977060
C	-2.639399700	-1.585826550	-0.951155610
C	-2.963785450	-3.930975720	-1.179386010
C	-2.968320180	1.356382960	3.431261210
C	-3.199431440	0.590837530	0.851522000
C	-3.482119880	-2.646754320	-1.230035310
C	-4.222305040	1.088017880	2.929011320
C	-4.352783620	0.701161050	1.611481730
H	0.029597700	-3.888147290	3.324007120
H	0.233578470	-3.082223930	-0.485873180
H	0.273486050	1.519768510	-4.036031720
H	0.862416640	-1.427908570	-2.968595280
H	1.156535610	0.238515100	2.972311890
H	1.171000340	5.095495310	0.891512200
H	1.731245090	-4.428291030	1.597745800
H	2.835027280	-1.683922140	-4.460654810
H	3.605470980	4.789364780	1.371700510
H	4.526469850	2.446631930	1.462381400
H	5.103846920	-1.192227180	-3.560022020
H	5.319257400	-0.504717310	-1.151334820
H	-0.029597700	3.888147290	-3.324007120
H	-0.233578470	3.082223930	0.485873180

H	-0.273486050	-1.519768510	4.036031720
H	-0.862416640	1.427908570	2.968595280
H	-1.156535610	-0.238515100	-2.972311890
H	-1.171000340	-5.095495310	-0.891512200
H	-1.731245090	4.428291030	-1.597745800
H	-2.835027280	1.683922140	4.460654810
H	-3.605470980	-4.789364780	-1.371700510
H	-4.526469850	-2.446631930	-1.462381400
H	-5.103846920	1.192227180	3.560022020
H	-5.319257400	0.504717310	1.151334820

Cartesian coordinates (Å) for S₀ state of bis-scorpionate [Ag(N,N',N"-Py₃PO)₂]⁺ cation.

Ag	0.107747000	0.300160000	-0.217424000
P	3.422153000	-0.657622000	1.085936000
P	-3.516367000	0.403635000	-0.905868000
O	4.782443000	-1.006031000	1.567970000
O	-4.969117000	0.491732000	-1.198508000
N	0.832621000	-1.239409000	1.792847000
N	1.943406000	1.663603000	0.791593000
N	2.000660000	-0.967280000	-1.261258000
N	-1.187162000	1.387594000	-2.035210000
N	-1.620557000	-1.581965000	-0.747493000
N	-1.861735000	1.056925000	1.197608000
C	0.233740000	-2.795316000	3.505195000
C	1.568276000	-3.065652000	3.757748000
C	1.762783000	2.973085000	0.945508000
C	1.881727000	-1.354389000	-2.528446000
C	2.115399000	-1.507839000	2.043538000
C	2.537144000	-2.408965000	3.012420000
C	2.703031000	3.808438000	1.532070000
C	2.926274000	-1.908974000	-3.254727000
C	3.093657000	1.140563000	1.228551000
C	3.187744000	-1.128874000	-0.669621000
C	3.892638000	3.258632000	1.977039000
C	4.096516000	1.895269000	1.823074000
C	4.153925000	-2.067949000	-2.635073000
C	4.292031000	-1.672874000	-1.312481000
C	-0.083831000	-1.876220000	2.513727000
C	-0.523208000	2.038450000	-2.987463000
C	-1.138477000	2.607984000	-4.093192000
C	-1.236196000	-2.853884000	-0.730539000
C	-1.619685000	1.581229000	2.395287000
C	-2.122769000	-3.916764000	-0.839954000
C	-2.512364000	2.499209000	-4.216643000
C	-2.514518000	1.285518000	-2.163694000
C	-2.595109000	2.201552000	3.163560000
C	-2.924697000	-1.328805000	-0.875536000
C	-3.107886000	1.134188000	0.723990000
C	-3.219441000	1.824880000	-3.231877000
C	-3.473655000	-3.643349000	-0.973914000
C	-3.883577000	2.280301000	2.662732000
C	-3.890347000	-2.320004000	-0.994238000
C	-4.152381000	1.732960000	1.416271000
H	0.551686000	2.107003000	-2.858990000
H	0.820053000	3.370416000	0.584570000
H	0.903829000	-1.216013000	-2.978120000
H	1.854522000	-3.775913000	4.523848000
H	2.498915000	4.866465000	1.631433000
H	2.771843000	-2.208190000	-4.283127000

H	3.595779000	-2.573036000	3.164489000
H	4.652269000	3.877819000	2.438008000
H	4.993269000	-2.496246000	-3.169045000
H	5.004815000	1.406652000	2.149768000
H	5.222838000	-1.780221000	-0.771565000
H	-0.170447000	-3.025107000	-0.619963000
H	-0.544705000	3.125738000	-4.834953000
H	-0.553775000	-3.284074000	4.063926000
H	-0.598928000	1.494621000	2.753230000
H	-1.116850000	-1.637891000	2.282759000
H	-1.754532000	-4.934223000	-0.821930000
H	-2.342397000	2.610058000	4.133274000
H	-3.029733000	2.932032000	-5.063896000
H	-4.195231000	-4.446155000	-1.063747000
H	-4.294544000	1.710203000	-3.269886000
H	-4.671426000	2.756982000	3.233019000
H	-4.930410000	-2.042085000	-1.102882000
H	-5.140350000	1.754327000	0.975837000

§9. Photophysical study

Photoluminescence spectra were recorded on a Fluorolog 3 spectrometer (Horiba Jobin Yvon) with a cooled PC177CE-010 photon detection module equipped with an R2658 photomultiplier. The luminescence decays and delayed luminescence spectra were measured on the same instrument. The absolute values of PLQYs were recorded using a Fluorolog 3 Quanta-phi device. The luminescence quantum yield at 77 K was obtained relative to the quantum yield of the same sample at 300 K. Independently, these relative quantum yields were calibrated by use of the absolute Φ_{PL} values measured at 77 K. Temperature dependences of luminescence were carried out using Optistat DN optical cryostats (Oxford Instruments).

The solid-state reflectance spectra were recorded on a Shimadzu UV-3101 spectrophotometer. Samples were prepared by a thorough grinding of a mixture of a complex (*ca.* 2 mol%) with BaSO₄. The reflectance data were converted into a spectrum applying a Kubelka–Munk function using BaSO₄ as a standard.

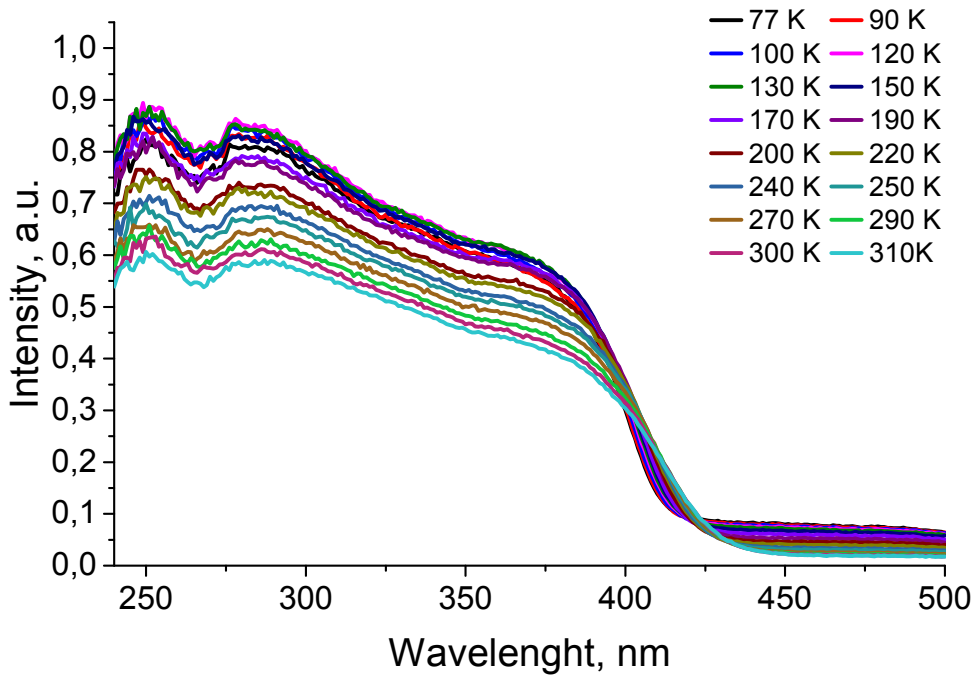


Fig. S25. Temperature dependence of excitation spectra of **1** at $\lambda_{\text{em}} = 580$ nm.

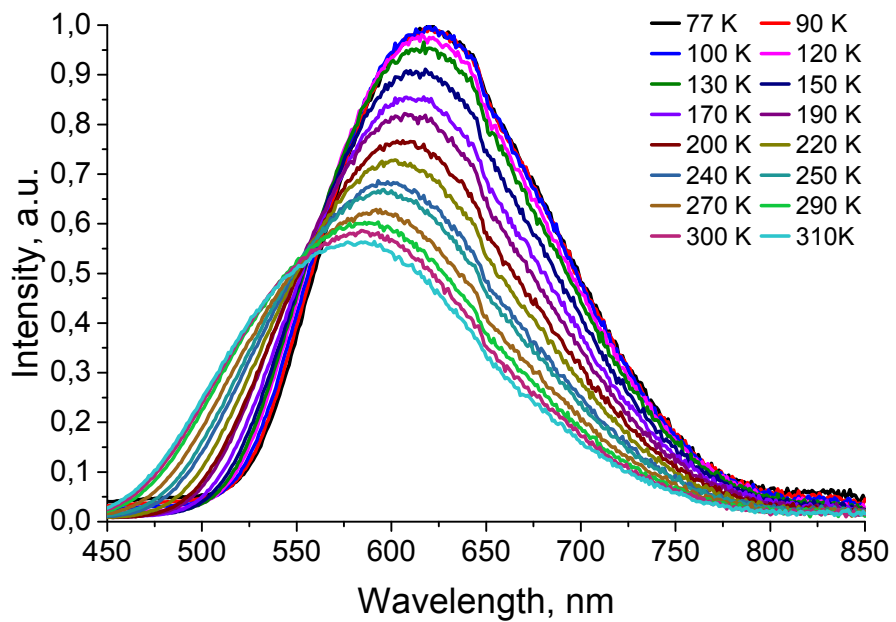


Fig. S26. Temperature-dependence of emission spectra of **1** recorded at $\lambda_{\text{ex}} = 300$ nm.

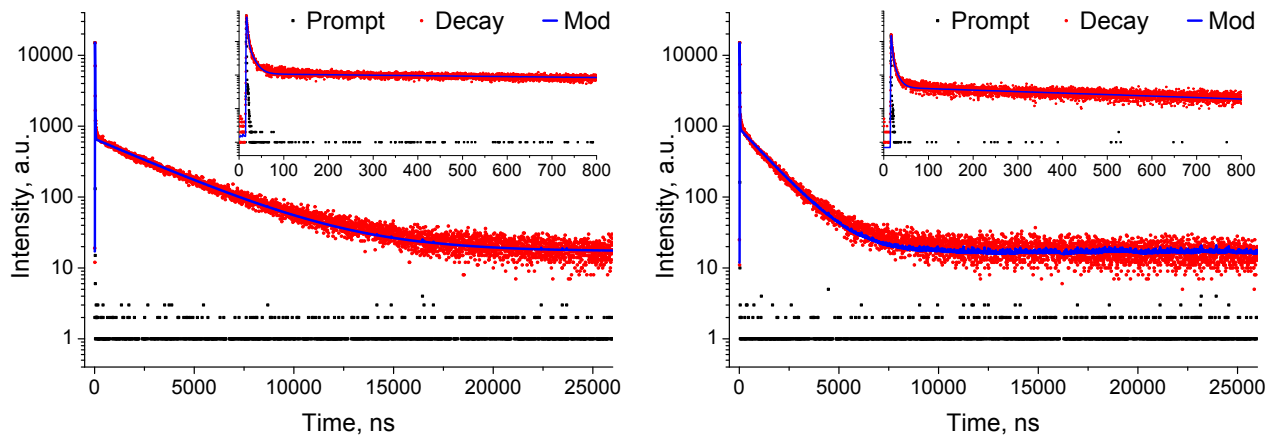


Fig. S27. Luminescence decay curves for **1** ($\lambda_{\text{ex}} = 350 \text{ nm}$, $\lambda_{\text{em}} = 600 \text{ nm}$) at 77 K (left) and 300 K (right).

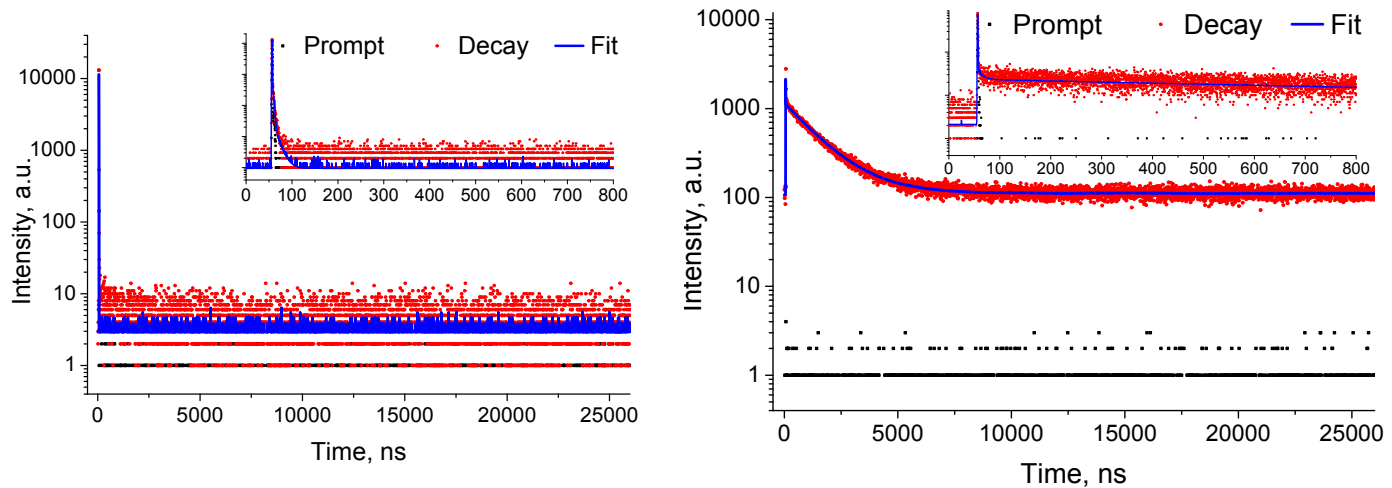


Fig. S28. Luminescence decay curves for **1** at 300 K ($\lambda_{\text{ex}} = 350 \text{ nm}$) recorded for $\lambda_{\text{em}} = 425 \text{ nm}$ (left) and $\lambda_{\text{em}} = 700 \text{ nm}$ (right).

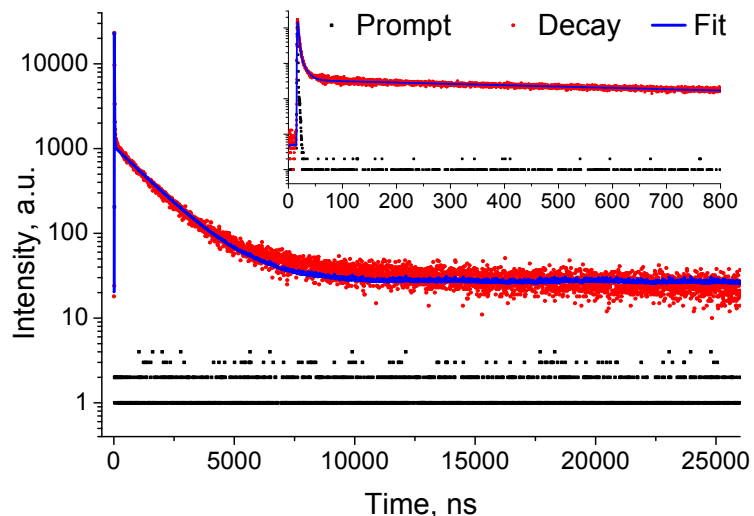


Fig. S29. Luminescence decay curves for **1** ($\lambda_{\text{ex}} = 300 \text{ nm}$, $\lambda_{\text{em}} = 600 \text{ nm}$) at 300 K.

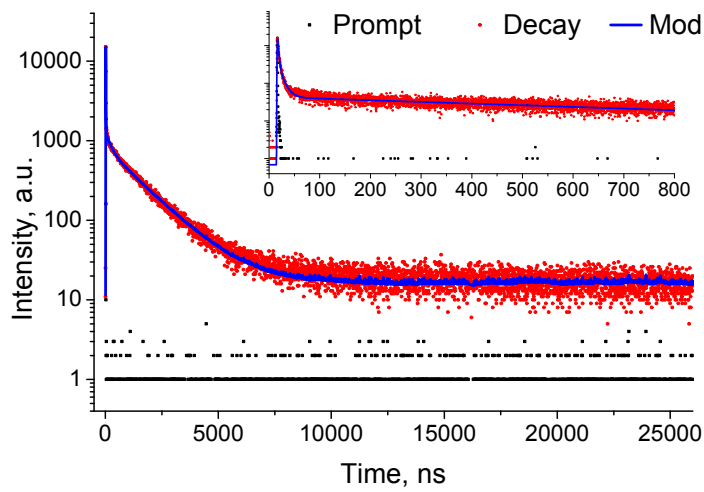


Fig. S30. Luminescence decay curves for **1** ($\lambda_{\text{ex}} = 350 \text{ nm}$, $\lambda_{\text{em}} = 600 \text{ nm}$) at 300 K.

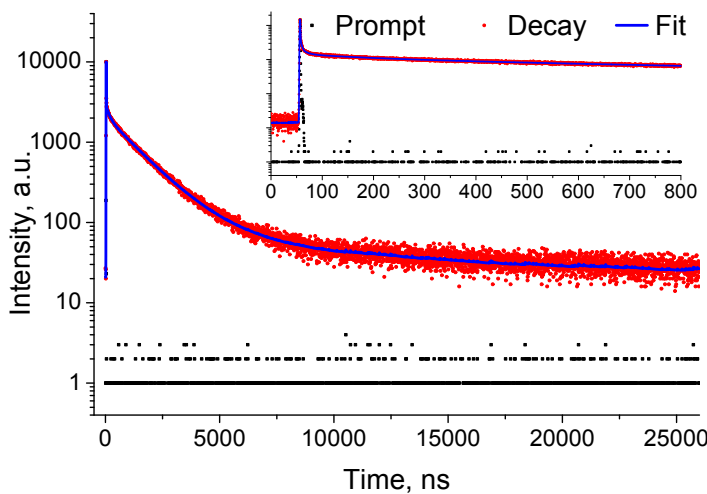


Fig. S31. Luminescence decay curves for **1** ($\lambda_{\text{ex}} = 390 \text{ nm}$, $\lambda_{\text{em}} = 600 \text{ nm}$) at 300 K.

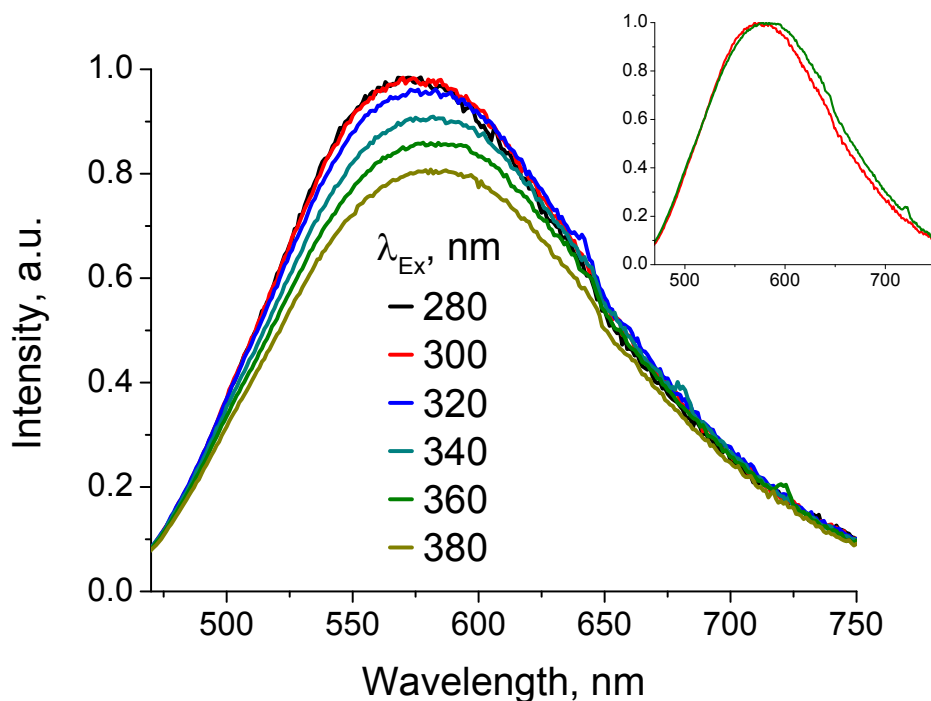


Fig. S32. Emission spectra of **1** recorded at various excitations ($\lambda_{\text{ex}} = 280\text{--}380 \text{ nm}$).

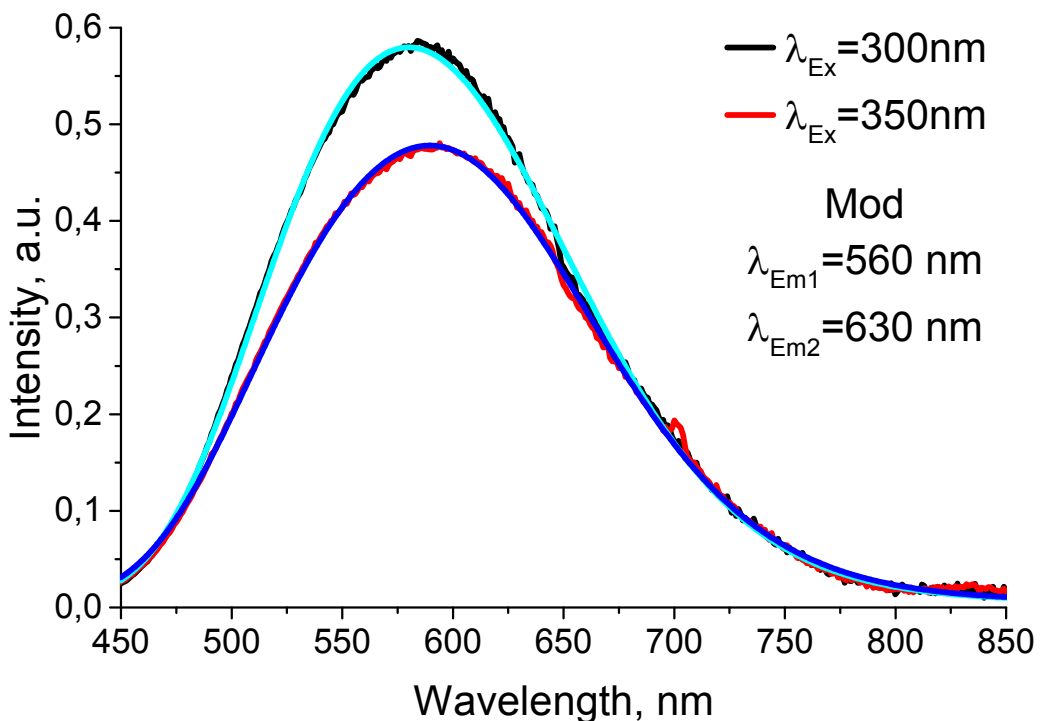


Fig. S33. Emission spectra of **1**: — and — are experimental spectra at 300 K, recorded at $\lambda_{\text{ex}} = 300$ and 350 nm, respectively; — and — are fitting spectra corresponding to the superposition of two Gauss functions with the maxima at $\lambda_1 \sim 560$ nm and $\lambda_2 \sim 630$ nm.

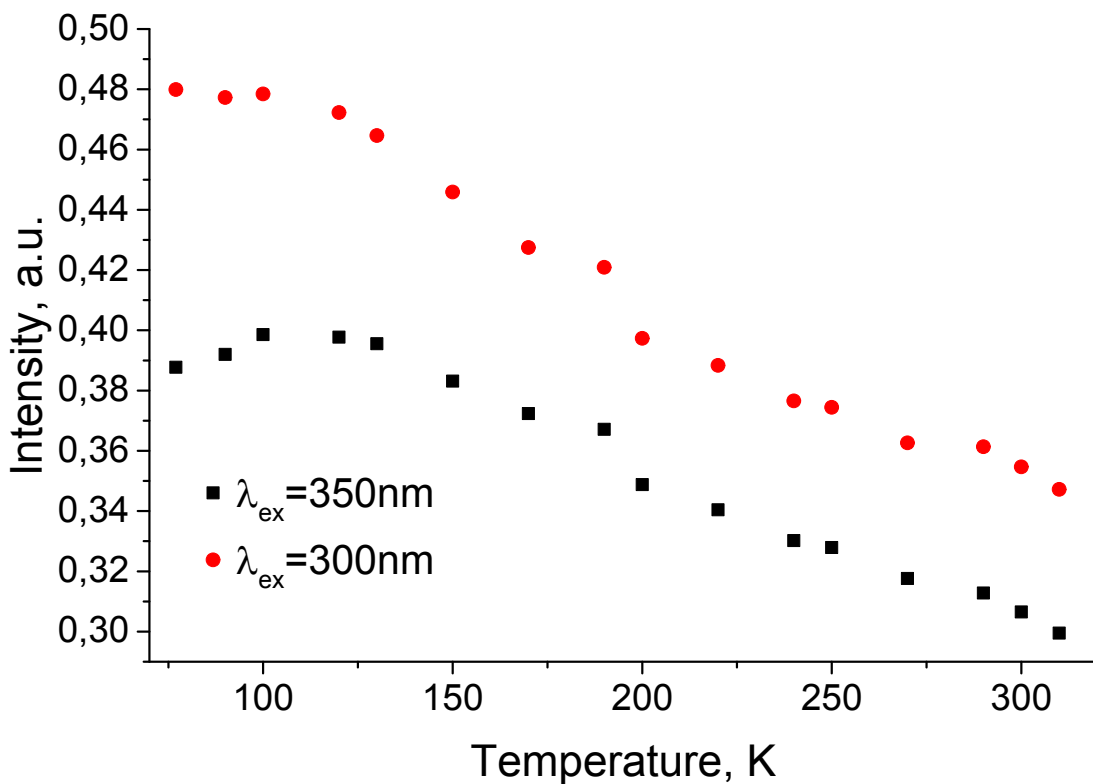


Fig. S34. Dependence of the integrated luminescence intensity as a function of temperature for complex **1** ($\lambda_{\text{ex}} = 300$ and 350 nm).

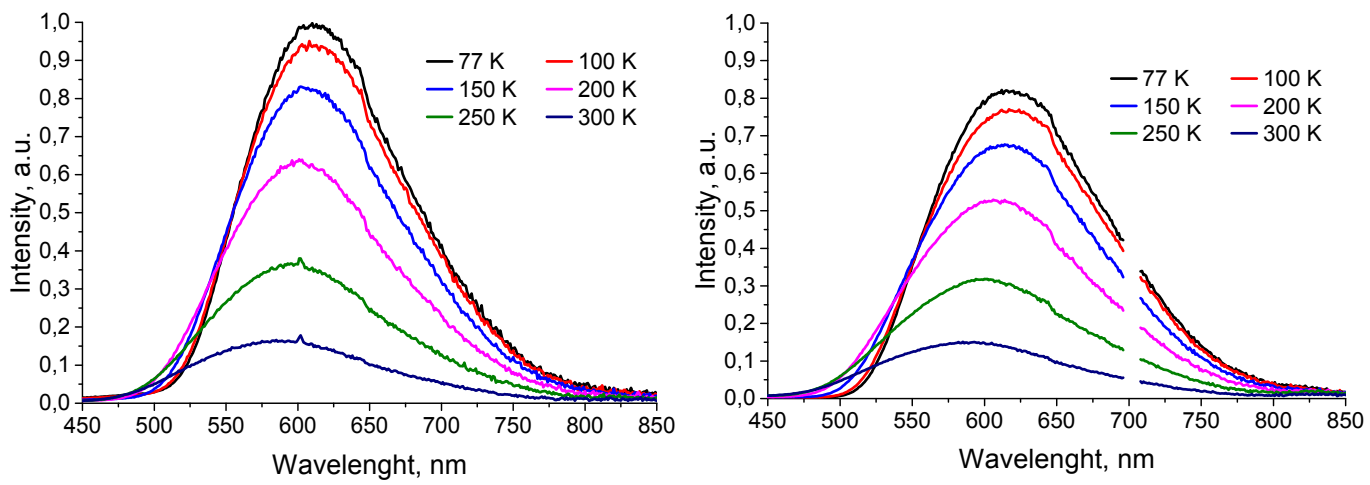


Fig. S35. Temperature dependence of emission spectra of **2** at $\lambda_{\text{ex}} = 300 \text{ nm}$ (*left*), $\lambda_{\text{ex}} = 350 \text{ nm}$ (*right*).

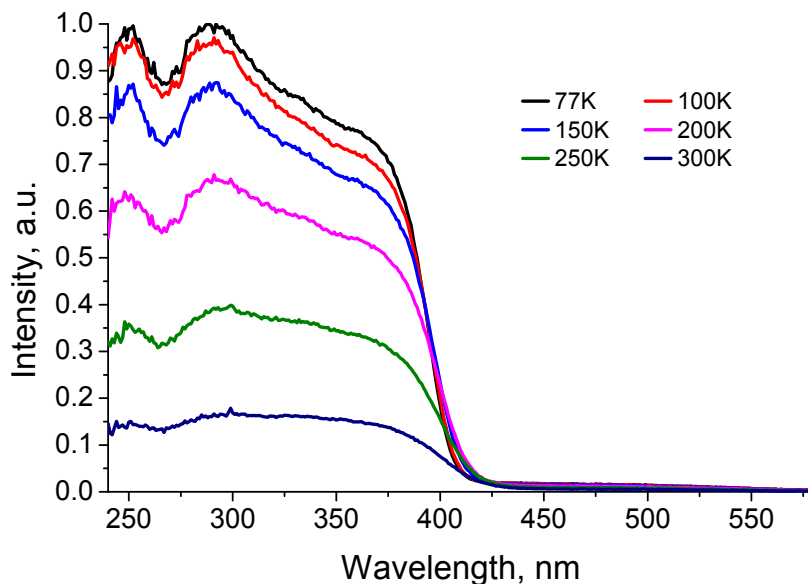


Fig. S36. Temperature dependence of the excitation spectra of **2** ($\lambda_{\text{em}} = 600 \text{ nm}$).

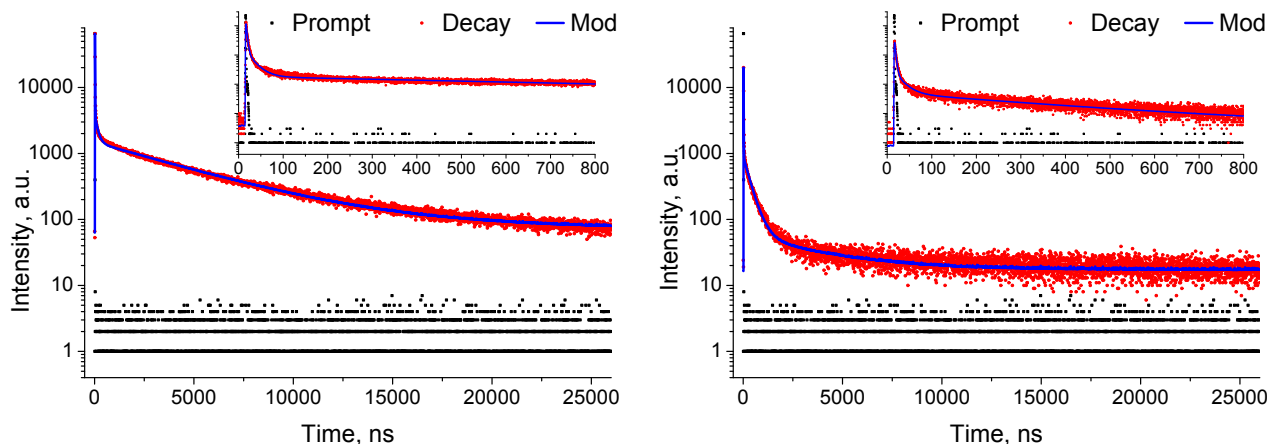


Fig. S37. Luminescence decay curves of **2** ($\lambda_{\text{ex}} = 350 \text{ nm}$, $\lambda_{\text{em}} = 600 \text{ nm}$) measured at 77 K (*left*) and 300 K (*right*).



Fig. S38. The powder of **2** under UV-light at 300 K (*left*) and \sim 80 K (*right*).

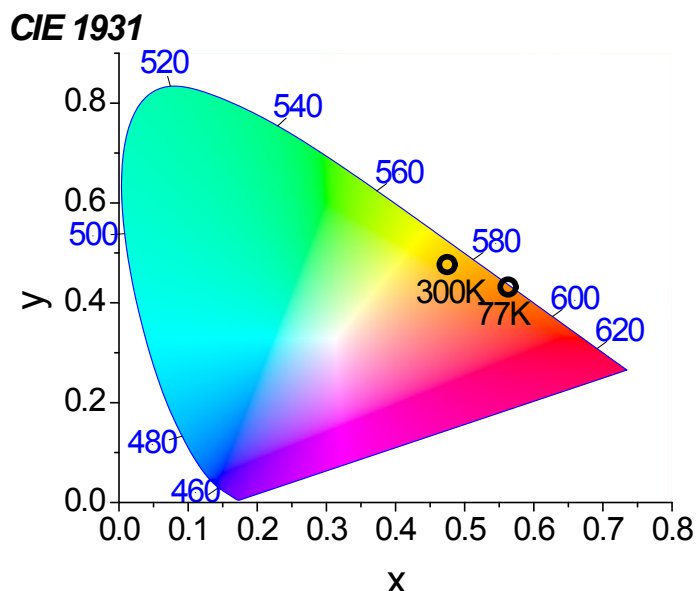


Fig. S39. CIE-1931 chromaticity diagram showing temperature dependence of the emission color of **2** ($\lambda_{\text{ex}} = 350$ nm).

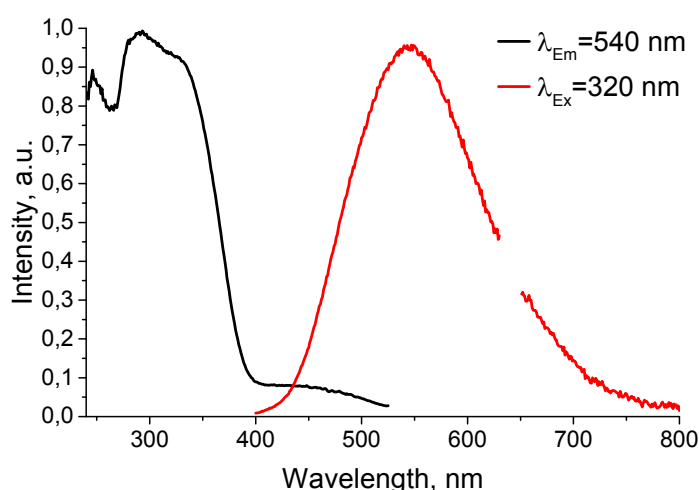


Fig. S40. Excitation ($\lambda_{\text{em}} = 540$ nm) and emission ($\lambda_{\text{em}} = 320$ nm) spectra of co-crystals **3** at 300 K.

§10. References

- [1] B.A. Trofimov, A.V. Artem'ev, S.F. Malysheva, N.K. Gusarova, N.A. Belogorlova, A.O. Korocheva, Yu.V. Gatilov, V.I. Mamatyuk, *Tetrahedron Lett.*, 2012, **53**, 2424–2427.
- [2] CrysAlisPro 1.171.38.46, Rigaku Oxford Diffraction, 2015.

- [3] G.M. Sheldrick *Acta Crystallogr.*, 2015, **A71**, 3–8.
- [4] G.M. Sheldrick, *Acta Crystallogr.*, 2015, **C71**, 3–8.
- [5] M. Swart, *Chem. Phys. Lett.*, 2013, **580**, 166–171.
- [6] J.P. Perdew, K. Burke, M. Ernzerhof, *Phys. Rev. Lett.*, 1996, **77**, 3865–3868.
- [7] J.P. Perdew, Y. Wang, *Phys. Rev.*, 1992, **B45**, 13244–13249.
- [8] E. van Lenthe, E.J. Baerends, *J. Comput. Chem.*, 2003, **24**, 1142–1156.
- [9] G. te Velde, F.M. Bickelhaupt, E.J. Baerends, C. Fonseca Guerra, S.J.A. van Gisbergen, J.G. Snijders, T. Ziegler, *J. Comput. Chem.*, 2001, **22**, 931–967.
- [10] C. Fonseca Guerra, J.G. Snijders, G. te Velde, E.J. Baerends, *Theor. Chem. Acc.*, 1998, **99**, 391–403.
- [11] ADF2017, SCM, Theoretical Chemistry, Vrije Universiteit, Amsterdam, The Netherlands, <http://www.scm.com>.
- [12] E. van Lenthe, A.E. Ehlers, E.J. Baerends, *J. Chem. Phys.*, 1999, **110**, 8943–8953.
- [13] S.J.A. van Gisbergen, J.G. Snijders, E.J. Baerends, *Comput. Phys. Commun.*, 1999, **118**, 119–138.
- [14] A. Rosa, E.J. Baerends, S.J.A. van Gisbergen, E. van Lenthe, J.A. Groeneveld, J. G. Snijders, *J. Am. Chem. Soc.*, 1999, **121**, 10356–10365.
- [15] A.D. Becke, K.E. Edgecombe, *J. Chem. Phys.*, 1990, **92**, 5397–5403.
- [16] B. Silvi, A. Savin, *Nature*, 1994, **371**, 683–686.
- [17] R.F.W. Bader, *Atoms in molecules: a quantum theory*, Oxford, Clarendon Press, 1990.
- [18] M. Kohout, DGrid, version 4.6, Radebeul, 2011.